Detailed analyses of the crucial functions of Zn transporter proteins in alkaline phosphatase activation

Received for publication, January 14, 2020, and in revised form, March 4, 2020 Published, Papers in Press, March 16, 2020, DOI 10.1074/jbc.RA120.012610

Eisuke Suzuki[‡1], Namino Ogawa[‡1], Taka-aki Takeda[‡1], Yukina Nishito[‡1], Yu-ki Tanaka[§], Takashi Fujiwara[¶], Mayu Matsunaga[‡], Sachiko Ueda[‡], Naoya Kubo[‡], Tokuji Tsuji[‡], Ayako Fukunaka[‖], Tomohiro Yamazaki[**], Kathryn M. Taylor[‡‡], Yasumitsu Ogra[§], and Taiho Kambe[‡2]

From the [‡]Graduate School of Biostudies, Kyoto University, Kyoto 606-8502, Japan, the [§]Graduate School of Pharmaceutical Sciences, Chiba University, Chiba 260-8675, Japan, the [¶]Graduate School of Bioagricultural Sciences, Nagoya University, Nagoya 464-8601, Japan, the [‖]Institute for Molecular and Cellular Regulation, Gunma University, 3-39-15 Showa-machi, Maebashi, Gunma 371-8512, Japan, the [**]Institute for Genetic Medicine, Hokkaido University, Sapporo 060-0815, Japan, and the [‡‡]School of Pharmacy and Pharmaceutical Sciences, Redwood Building, Cardiff University, King Edward VIIth Avenue, Cardiff CF10 3NB, United Kingdom

Edited by Mike Shipston

Numerous zinc ectoenzymes are metalated by zinc and activated in the compartments of the early secretory pathway before reaching their destination. Zn transporter (ZNT) proteins located in these compartments are essential for ectoenzyme activation. We have previously reported that ZNT proteins, specifically ZNT5–ZNT6 heterodimers and ZNT7 homodimers, play critical roles in the activation of zinc ectoenzymes, such as alkaline phosphatases (ALPs), by mobilizing cytosolic zinc into these compartments. However, this process remains incompletely understood. Here, using genetically-engineered chicken DT40 cells, we first determined that Zrt/Irt-like protein (ZIP) transporters that are localized to the compartments of the early secretory pathway play only a minor role in the ALP activation process. These transporters included ZIP7, ZIP9, and ZIP13, performing pivotal functions in maintaining cellular homeostasis by effluxing zinc out of the compartments. Next, using purified ALP proteins, we showed that zinc metalation on ALP produced in DT40 cells lacking ZNT5–ZNT6 heterodimers and ZNT7 homodimers is impaired. Finally, by genetically disrupting both ZNT5 and ZNT7 in human HAP1 cells, we directly demonstrated that the tissue-nonspecific ALP-activating functions of both ZNT complexes are conserved in human cells. Furthermore, using mutant HAP1 cells, we uncovered a previously-unrecognized and unique spatial regulation of ZNT5–ZNT6 heterodimer formation, wherein ZNT5 recruits ZNT6 to the Golgi apparatus to form the heterodimeric complex. These findings fill in major gaps in our understanding of the molecular mechanisms underlying zinc ectoenzyme activation in the compartments of the early secretory pathway.

Zn transporter (ZNT)[3] family proteins, except ZNT1 and ZNT10 (1–3), localize to specific subcellular compartments and perform unique functions (4, 5). ZNT2, ZNT3, and ZNT8, which localize to regulatory secretory vesicles/granules in specialized cells, play pivotal roles in the specific physiological functions of these cells (6–13) in distinct manners (14–16); conversely, ZNT5, ZNT6, and ZNT7, which localize to the compartments of the early secretory pathway in generic cells, play general but key roles in the cells (17–19). One of these roles of ZNT proteins is their critical function of supplying zinc to numerous proteins, including several secretory, extracellularly membrane-bound or organelle-resident enzymes biosynthesized in the compartments (hereafter zinc ectoenzymes), for their activation (20, 21). In this context, we have shown that vertebrate ZNT5–ZNT6 heterodimers and ZNT7 homodimers are required for the activation of alkaline phosphatases (ALPs), such as tissue-nonspecific ALP (TNAP) (22) and placental ALP (PLAP) (23), and several other ectoenzymes by using genetically-engineered chicken DT40 cell mutants (24–27).

Compared with the elucidation of the importance of ZNT proteins in zinc ectoenzyme activation, the involvement of another family of zinc transporter proteins, Zrt/Irt-like proteins (ZIPs), in the activation remains less well-studied (20, 21). However, certain ZIPs have recently been clearly shown to play several pivotal roles in early secretory pathway functions (28–

This work was supported by Grant-in-aid for Scientific Research on Innovative Areas "Bio-metal" KAKENHI Grants 19H05768 (to T. K.) and 19H05772 (to Y. O.) from the Ministry of Education, Culture, Sports, Science, and Technology, Japan; Grant-in-aid for Scientific Research (B) KAKENHI Grants 15H04501 and 19H02883 (to T. K.) from the Japan Society for the Promotion of Science; Grant-in-aid for JSPS Research Fellows KAKENHI Grants 17J06767 (to T. Takeda) and 17J09455 (to Y. N.); the Fuji Foundation for Protein Research; the Salt Science Research Foundation; the Takeda Science Foundation; the Kieikai Research Foundation; the Ito Foundation; Sugiyama Chemical and Industrial Laboratory; the Kao Melanin Workshop; the Cosmetology Research Foundation; the Kyoto Innovative Medical Technology Research and Development Support System; and the Mitsubishi Foundation (to T. K.). The authors declare that they have no conflicts of interest with the contents of this article.
This article contains Figs. S1–S4 and Tables S1–S3.

[1] These authors contributed equally to this work.

[2] To whom correspondence should be addressed: Division of Life Science, Graduate School of Biostudies, Kyoto University, Kyoto 606-8502, Japan. Tel: +81-75-753-6273; Fax: +81-75-753-6274; E-mail: kambe1@kais.kyoto-u.ac.jp.

[3] The abbreviations used are: ZNT, Zn transporter; HA, hemagglutinin; TKO, triple knockout; ZIP, Zrt/Irt-like protein; DKO, double knockout; GPI, glycosylphosphatidylinositol; ANOVA, analysis of variance; ALP, alkaline phosphatase; DAPI, 4,6-diamino-2-phenylindole; Cnx, calnexin; PLAP, placental ALP; ER, endoplasmic reticulum; CALR, calreticulin; TNAP, tissue-nonspecific ALP; FCS, fetal calf serum; secPLAP, secreted form of PLAP; sup, supernatant; ICP-MS, inductively coupled plasma-mass spectrometry.

Downloaded from http://www.jbc.org/ at Kyoto University on June 11, 2020

© 2020 Suzuki et al. Published under exclusive license by The American Society for Biochemistry and Molecular Biology, Inc.

31). Specifically, ZIP7, ZIP9, and ZIP13 participate in zinc mobilization from the luminal side to the cytosol and contribute to the homeostatic maintenance of early secretory pathway functions, including those of the ER and Golgi apparatus (29, 30, 32–34), in addition to performing crucial functions in zinc signaling by regulating signal transduction pathways in response to various stimuli (35–38). These critical functions of ZIPs suggest that these proteins might contribute to the process underlying the activation of zinc ectoenzymes, including ALPs.

The ability of ZNT5–ZNT6 heterodimers and ZNT7 homodimers to activate TNAP has been shown to be conserved in other species, such as *Caenorhabditis elegans* (in which ZNT5 and ZNT6 are named Cdf5 and Toc1, respectively) (39), by using the DT40 cell system. However, we have not yet obtained direct evidence indicating that human cells lacking both ZNT complexes show similar defects in ALP activation as in the case of DT40 cells. In this study, we investigated this fundamental question and other related questions by performing various biochemical experiments on chicken DT40 cells and human HAP1 cells. Addressing these questions can deepen our understanding of the activation process of zinc ectoenzymes in the compartments of the early secretory pathway.

Results

Alteration of ZIP expression does not markedly affect Tnap activation

To examine how ZIPs localized to the early secretory pathway contribute to the TNAP activation process, we established DT40 cells deficient in *zip13* (*zip13*$^{-/-}$) or both *zip9* and *zip13* (*zip9*$^{-/-}$*zip13*$^{-/-}$) (Fig. S1). This is because we already established *zip9*$^{-/-}$ cells in our previous study (33), in which *zip13* mRNA expression was increased (Fig. 1*A*). The ortholog of ZIP7, another ZIP localized to the early secretory pathway, is not encoded by the chicken genome (40), which precluded the establishment of DT40 cells deficient in *Zip7*. Tnap activity in *zip9*$^{-/-}$, *zip13*$^{-/-}$, and *zip9*$^{-/-}$*zip13*$^{-/-}$ cells was not markedly decreased (Fig. 1*A*), and in zinc-deficient cultures, Tnap activity in *zip9*$^{-/-}$*zip13*$^{-/-}$ cells, as in WT cells, was almost eliminated (Fig. 1*B*). Re-expression of ZIP9 or ZIP13 in *zip9*$^{-/-}$*zip13*$^{-/-}$ cells also did not alter Tnap activity as compared with the activity in WT and in *zip9*$^{-/-}$*zip13*$^{-/-}$ cells (Fig. 1*C*). To comprehensively investigate the functions of Zip9 and Zip13 in Tnap activation, we disrupted both metallothionein I and II (*mtI* and *mtII*, hereafter *mt*) in *zip9*$^{-/-}$*zip13*$^{-/-}$ cells and thus generated *mt*$^{-/-}$*zip9*$^{-/-}$*zip13*$^{-/-}$ cells; we did this because metallothioneins can chelate cytosolic zinc (41, 42), and *mt* disruption in cells could thus drastically alter cellular zinc homeostasis. However, we found that Tnap activity in *mt*$^{-/-}$*zip9*$^{-/-}$*zip13*$^{-/-}$ cells was not altered relative to that in WT cells and *zip9*$^{-/-}$*zip13*$^{-/-}$ cells (Fig. 1*D*).

ZIP7 has recently been reported to play a key role in zinc mobilization from the lumen of the ER (29–31), and the zinc-transport activity of ZIP7 has further been reported to be facilitated by its phosphorylation by CK2 (37). To examine ZIP7 involvement in Tnap activation, we ectopically expressed WT ZIP7 or mutant ZIP7, either the phosphoablative form or the phosphomimetic active form (ZIP7$_{S275A/S276A}$ or ZIP7$_{S275D/S276D}$) (37, 43), in *zip9*$^{-/-}$*zip13*$^{-/-}$ cells (Fig. 1*E*). Expression of neither WT ZIP7 nor ZIP7$_{S275A/S276A}$ markedly altered Tnap activity in *zip9*$^{-/-}$*zip13*$^{-/-}$ cells, whereas the expression of ZIP7$_{S275D/S276D}$ decreased Tnap activity by ~40% (Fig. 1*E*). Moreover, zinc supplementation did not produce any changes in Tnap activity here (Fig. 1*F*), which excluded the possibility that ZIP7$_{S275D/S276D}$ expression decreased zinc levels in the lumen of the compartments of the early secretory pathway; this suggests that ZIP7$_{S275D/S276D}$ expression exerted its effect independently of the zinc-mobilization ability of the protein.

We next examined whether disruption of both *zip9* and *zip13* in *znt5*$^{-}$*znt6*$^{-/-}$*znt7*$^{-/-}$ (triple knockout; TKO) cells altered their reduced Tnap activity phenotype. DT40 cells deficient in all of these genes, *i.e.* deficient in *znt5*, *znt6*, *znt7*, *zip9*, and *zip13* (TKO*zip9*$^{-/-}$*zip13*$^{-/-}$ cells), showed drastically-diminished Tnap activity much like TKO cells (Fig. 2*A*). Co-expression of ZNT5 and ZNT6 or re-expression of ZNT7 in TKO*zip9*$^{-/-}$*zip13*$^{-/-}$ cells reversed this loss of Tnap activity (Fig. 2*B*). Moreover, time-course experiments revealed the distinct contributions of ZIP and ZNT proteins to Tnap activation; from measurements of Tnap activity, the absorbance at 405 nm in both TKO cells and TKO*zip9*$^{-/-}$*zip13*$^{-/-}$ cells was found not to be saturated for up to 240 min, whereas that in *zip9*$^{-/-}$*zip13*$^{-/-}$ cells, TKO*zip9*$^{-/-}$*zip13*$^{-/-}$ cells stably co-expressing ZNT5 and ZNT6, and TKO*zip9*$^{-/-}$*zip13*$^{-/-}$ cells stably expressing ZNT7 was saturated by 120 min. This suggests that Tnap activity was drastically decreased in cells lacking Znt proteins as compared with that in Zip-deficient cells (Fig. 2*C*). These results clearly confirmed that ZNT5–ZNT6 heterodimers and ZNT7 homodimers play indispensable roles in TNAP activation, but that ZIPs, such as ZIP9 and ZIP13, play only minor roles.

Plant ZNT5–ZNT6 orthologs can activate Tnap

We previously showed that the function of ZNT5–ZNT6 heterodimers in Tnap activation is conserved in nematode orthologs by using the TKO cells (39). The conservation of this key function was further examined by expressing plant ZNT5 and ZNT6 orthologs, Mtp12 and Mtp5, in TKO cells. The results of co-immunoprecipitation experiments showed functional interaction between Mtp12 and Mtp5 and between Mtp12 and a splicing variant of Mtp5 (svMtp5, named Mtp5t2 in a previous study (44)) in TKO cells (Fig. 3*A*). Tnap activity was restored only following the co-expression of hemagglutinin (HA)- or FLAG-tagged Mtp12 and Mtp5 (Fig. 3*B*), as expected from the results of the previous zinc-transport study (44), and both of these proteins were co-localized in the Golgi apparatus in TKO cells (Fig. 3*C*). Notably, this restoration of Tnap activity was abolished following the replacement of histidine or aspartic acid with alanine in the putative transmembranous zinc-binding site of Mtp12 (Mtp12$_{H452A}$ and Mtp12$_{D666A}$), which probably generates loss-of-function mutants (Fig. 3*D*). Moreover, the restoration of Tnap activity by Mtp12–Mtp5 heterodimers was partial as compared with that mediated by ZNT5–ZNT6 co-expression, even when untagged Mtp12 and Mtp5 were used (Fig. 3*E*); this might reflect the effect of a single Pro residue in the PP-motif in luminal loop 2 of Mtp12, because the loss of one Pro residue in ZNT5 leads to reduced ability for Tnap acti-

Downloaded from http://www.jbc.org/ at Kyoto University on June 11, 2020

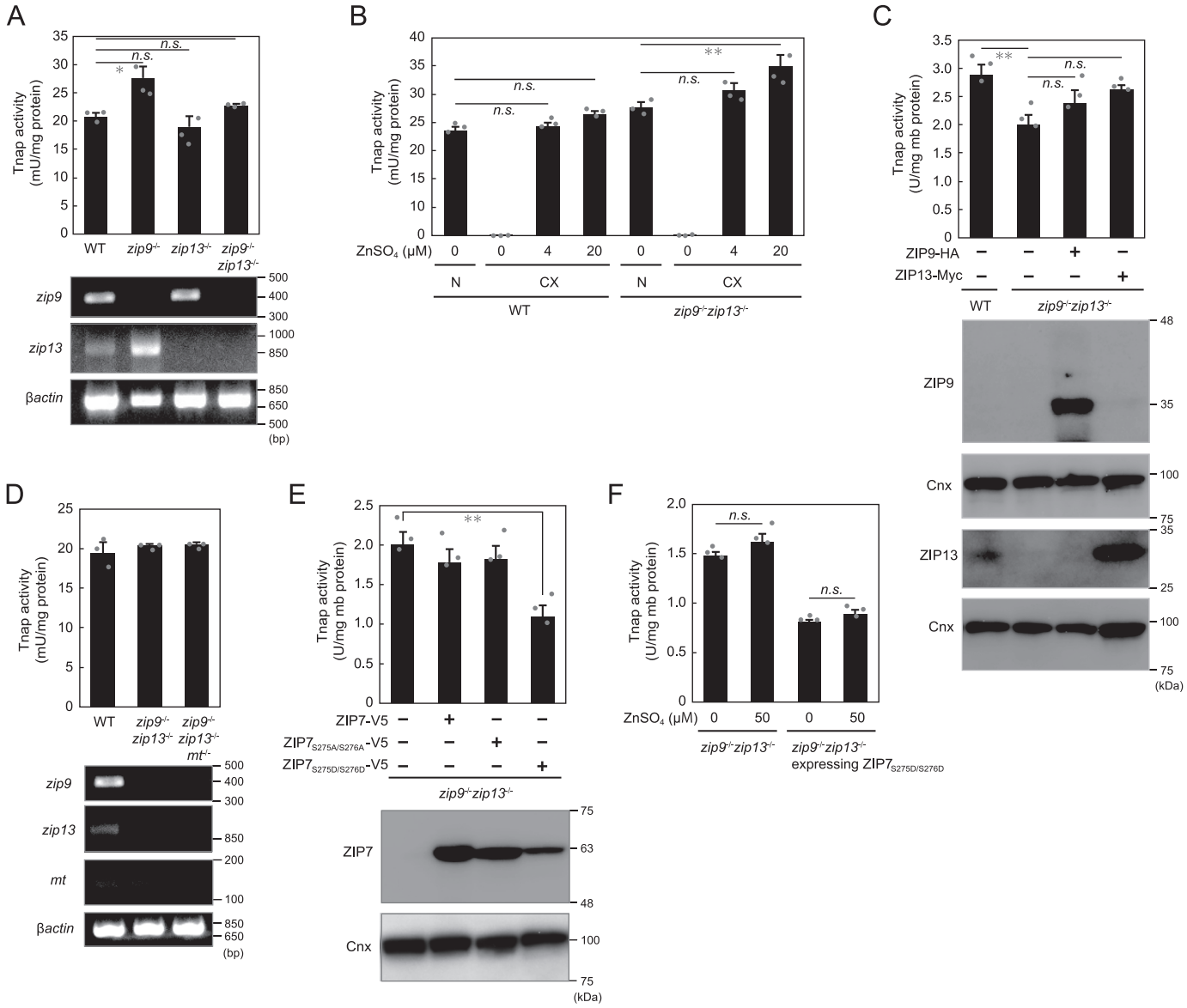

Figure 1. Alteration of expression of ZIPs localized to early secretory pathway does not markedly affect Tnap activity. *A*, Tnap activity was not substantially altered by the disruption of *zip9* or *zip13* or both genes (*zip9*$^{-/-}$*zip13*$^{-/-}$). *B*, in zinc-deficient cultures (*CX*), Tnap activity was potently suppressed in *zip9*$^{-/-}$*zip13*$^{-/-}$ cells, similarly as in WT cells. *N*, normal culture. *C*, re-expression of ZIP9 or ZIP13 did not notably affect Tnap activity in *zip9*$^{-/-}$*zip13*$^{-/-}$ cells. *D*, disruption of metallothionein genes (*mt*) in *zip9*$^{-/-}$*zip13*$^{-/-}$ cells did not alter Tnap activity. *E*, overexpression of WT ZIP7 or ZIP7 phosphoablative mutant (ZIP7$_{S275A/S276A}$) did not produce a large effect on Tnap activity, whereas the expression of the ZIP7 phosphomimetic active mutant (ZIP7$_{S275D/S276D}$) decreased (but did not eliminate) Tnap activity by ~40%. *F*, Tnap activity in *zip9*$^{-/-}$*zip13*$^{-/-}$ cells or in *zip9*$^{-/-}$*zip13*$^{-/-}$ cells stably expressing the ZIP7$_{S275D/S276D}$ mutant was not markedly changed by zinc supplementation. *A*, *B*, and *D*, Tnap activity was measured using total cellular proteins. *A–F*, all activities are expressed as means ± S.D. of triplicate experiments ($n = 3$). Statistical significance was analyzed by one-way ANOVA followed by Tukey's post hoc test in *A–C* or by Student's *t* test in *E* and *F*. *, $p < 0.05$; **, $p < 0.01$; *n.s.*, not significant. Calnexin (*Cnx*) was used as the loading control; *mb protein*, membrane protein. Each experiment was performed at least three times, and representative results from independent experiments are displayed.

vation (39). These results indicate that the Tnap activation ability is highly-conserved in ZNT5–ZNT6 orthologs, including those from plants, although the plant orthologs are relatively less effective in Tnap activation.

ZNT5–ZNT6 heterodimers and ZNT7 homodimers are required for proper zinc metalation of ALPs

ZNT5–ZNT6 heterodimers and ZNT7 homodimers play essential roles in TNAP activation; however, how TNAP protein is affected when expressed in the TKO cells was unclear. We addressed this question by using PLAP, an isozyme of TNAP, as a model, because we found that the secreted form of PLAP (secPLAP), which lacks the glycosylphosphatidylinositol (GPI) anchor (45), was not degraded when stably expressed in TKO cells (Fig. 4, *A* and *B*). By contrast, PLAP, when stably expressed in TKO cells, was degraded through cellular lysosomal and proteasomal degradation pathways (Fig. 4, *C–E*) similarly as TNAP (25). The ZNT-complex– dependence of PLAP activity was not noticeably altered between secPLAP and PLAP when expressed in TKO cells (Fig. 4, *B* and *D*), which indicates that secPLAP is likely present in an apo-form in TKO cells. Thus, we stably expressed C-terminally HA-tagged secPLAP (secPLAP–HA) (46) in WT and TKO cells (Fig. 4*F*), and we purified the protein from both cells by using anti-HA–tag

Downloaded from http://www.jbc.org/ at Kyoto University on June 11, 2020

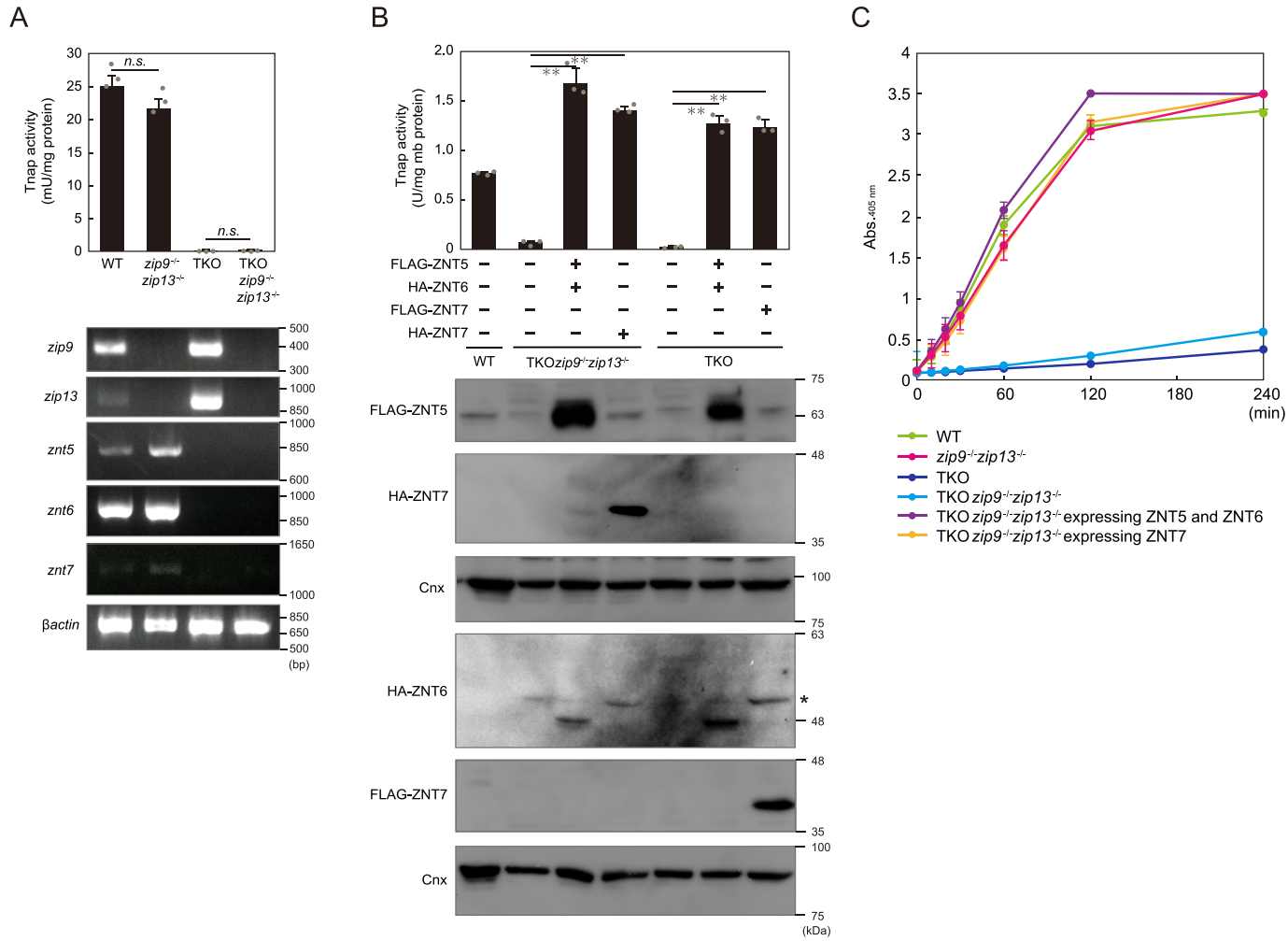

Figure 2. Minor contribution of ZIP9 and ZIP13 to Tnap activation process, compared with ZNT5–ZNT6 heterodimers and ZNT7 homodimers. *A,* TNAP activity relative to that in WT cells was not changed in *zip9*$^{-/-}$*zip13*$^{-/-}$ cells as compared with the activity in TKO and TKO*zip9*$^{-/-}$*zip13*$^{-/-}$ cells (*upper graph*). Tnap activity was measured using total cellular proteins. Confirmation of loss of *znt5*, *znt6*, *znt7*, *zip9*, and *zip13* mRNA expression in TKO*zip9*$^{-/-}$*zip13*$^{-/-}$ cells is shown in the *lower panels*. *B,* lack of both Zip9 and Zip13 did not impair the restoration of Tnap activity mediated by ZNT5–ZNT6 heterodimers or ZNT7 homodimers in TKO*zip9*$^{-/-}$*zip13*$^{-/-}$ cells. Cnx was used as the loading control. *, nonspecific band. *C,* comparison of the effects of lack of Zip or Znt proteins on Tnap activity in DT40 cells. *A* and *B,* measured Tnap activity is shown as means ± S.D. of triplicate experiments ($n = 3$). Statistical significance was analyzed by Student's *t* test in *A* or by one-way ANOVA followed by Tukey's post hoc test in *B*. **, $p < 0.01$; *n.s.*, not significant. Each experiment was performed at least three times, and representative results from independent experiments are presented.

antibody (see under "Experimental procedures") (Fig. S2). The activity of secPLAP–HA purified from TKO cells was substantially lower than that of the protein from WT cells (Fig. 4*G*), which agrees with the activity measured before purification (Fig. 4*F*). ICP-MS analysis revealed that the relative zinc content in secPLAP–HA purified from TKO cells was drastically lower than that in the protein purified from WT cells (Fig. 4*H*), suggesting that zinc metalation of secPLAP–HA was impaired in TKO cells. Furthermore, ALP zymography and immunoblotting performed using native-polyacrylamide gels failed to reveal the activity or the protein of secPLAP–HA purified from TKO cells at the corresponding positions as those of the protein from WT cells (Fig. 4*I*), although the proteins were detected at the same positions when immunoblotting was performed after SDS-PAGE (Fig. 4, *A* and *B*); this indicates that secPLAP–HA purified from TKO cells might not be properly folded. These results clearly show that by supplying zinc to ALPs such as PLAP, ZNT5–ZNT6 heterodimers and ZNT7 homodimers play indispensable roles in the expression of ALP activity.

Conserved TNAP-activation functions of ZNT5–ZNT6 heterodimers and ZNT7 homodimers in human cells

We have shown that ZNT5–ZNT6 heterodimers and ZNT7 homodimers are indispensable for the activation of several zinc ectoenzymes, including TNAP and PLAP, by using genetically-engineered chicken DT40 cells (24–27). However, a fundamental question that has remained unanswered is whether this holds true for mammalian cells, including human cells. We addressed this question by establishing cultured human cells lacking ZNT5–ZNT6 heterodimers and ZNT7 homodimers; we disrupted *ZNT5* and/or *ZNT7* by using the CRISPR/Cas9 system, and we used HAP1 cells for these studies because these cells exhibit zinc-dependent TNAP activity (Fig. 5*A*) (27) in addition to their unique haploid phenotype. TNAP activity was not substantially decreased in *ZNT5* or *ZNT7* KO HAP1 cells

Downloaded from http://www.jbc.org/ at Kyoto University on June 11, 2020

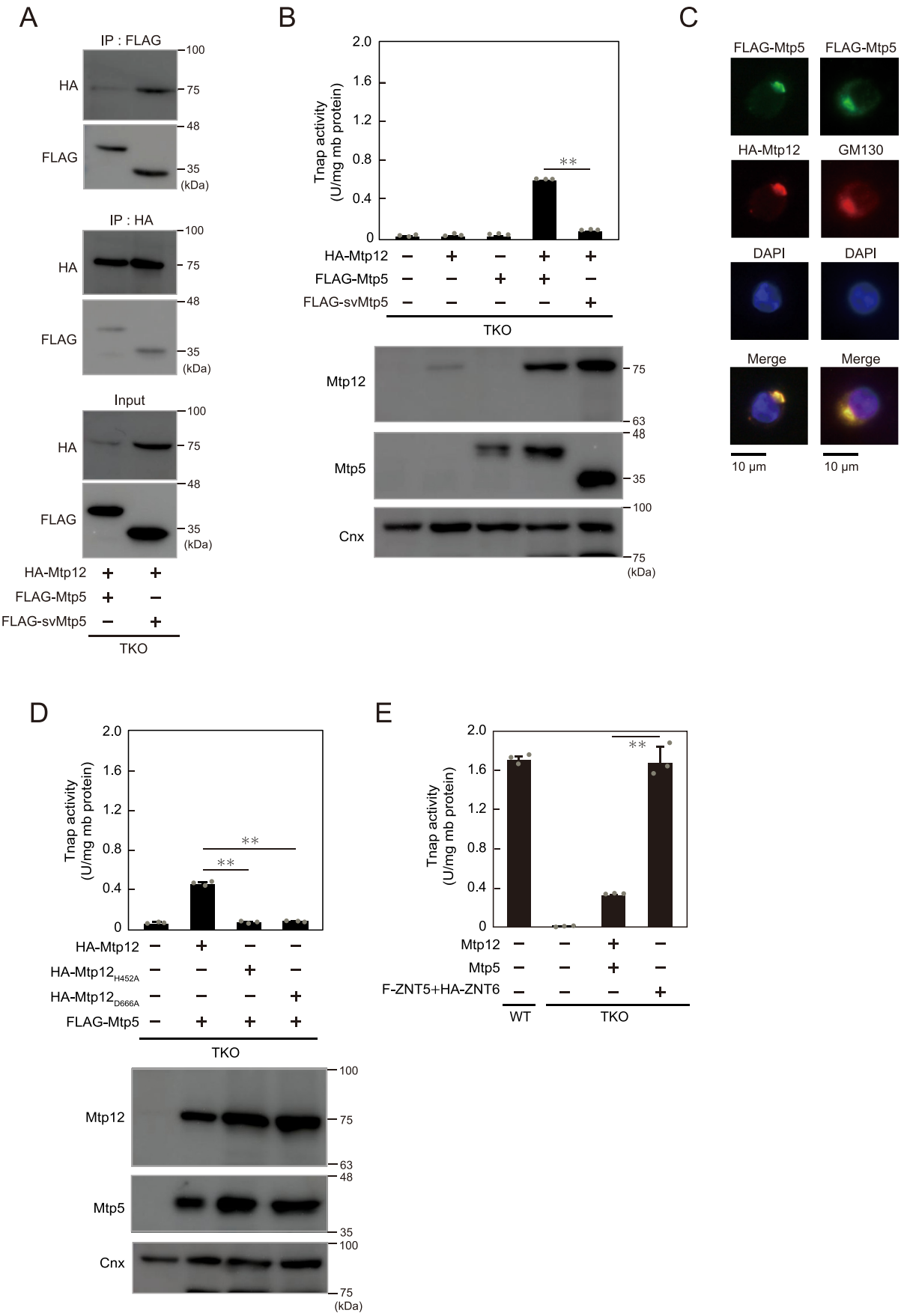

Downloaded from http://www.jbc.org/ at Kyoto University on June 11, 2020

(HAP–*Z5*-KO or HAP–*Z7*-KO cells) (Fig. 5*B* and Fig. S3), unlike in the case of DT40 cells, in which the activity was decreased by 45–60 and 20–30%, respectively, after *Znt5* and *Znt7* KO (24, 47). However, in *ZNT5* and *ZNT7* DKO cells (HAP–*Z5Z7*-DKO cells), TNAP activity was markedly decreased together with a decrease in protein expression (Fig. 5*B*), as in the case of DT40 cells lacking both *Znt5* and *Znt7* and in the TKO cells (24, 47). We confirmed this requirement of the disruption of both *ZNT5* and *ZNT7* for decreasing TNAP activity by using differently-generated HAP1 cells deficient in *ZNT5* and/or *ZNT7* (HAP–*Z7*-KO$_{(new)}$ and HAP–*Z5Z7*-DKO$_{(new)}$) (Fig. 5*C* and Fig. S1). Immunofluorescence staining revealed the loss of TNAP cell-surface localization in HAP–*Z5Z7*-DKO cells (Fig. 5*D*), which was also confirmed by the results of cell-surface biotinylation assays (Fig. 5*E*). TNAP was degraded through both the lysosomal and the proteasomal degradation pathways in HAP–*Z5Z7*-DKO cells, because the decreased TNAP protein expression in HAP–*Z5Z7*-DKO cells was partially restored (in terms of both the glycosylated size and the immature size) when cultured in the presence of lysosomal and proteasomal inhibitors (Fig. 5*F*). Moreover, we confirmed that ZNT5 and ZNT7 were essential for zinc ectoenzyme activation by stably overexpressing TNAP and PLAP. As expected, overexpressed TNAP and PLAP exhibited little activation in HAP–*Z5Z7*-DKO cells as compared with the enzymes expressed in WT HAP1 cells (Fig. 5, *G* and *H*). Accompanying this marked reduction in activity, TNAP and PLAP protein expression in HAP–*Z5Z7*-DKO cells was undetectable in immunoblotting assays (Fig. 5, *G* and *H*, *lane 5*), although both proteins were detected in WT cells even when cultured under zinc-deficient conditions (Fig. 5, *G* and *H*, *lane 3*); this is in accord with our present and previous results obtained using DT40 cell systems (27, 48).

The decrease in activity and loss of protein expression of TNAP were reversed by re-expression of ZNT5 or ZNT7 (Fig. 6*A*). Besides the re-expression of these human proteins, re-expression of the chicken orthologs in HAP–*Z5Z7*-DKO cells also restored TNAP activity and protein expression (Fig. 6*B*), which indicates complete compatibility between the human and chicken cellular systems in terms of TNAP activation by ZNT proteins. Concomitantly with this restoration, re-expression of ZNT5 or ZNT7 also fully rescued the cell-surface expression of TNAP (Fig. 6, *C* and *D*). However, TNAP activity was not restored by zinc supplementation in the culture medium of HAP–*Z5Z7*-DKO cells (Fig. 6*E*) nor by stable expression of the zinc transport–incompetent ZNT5$_{H451A}$ mutant (Fig. 6*F*). These results indicate that ZNT5–ZNT6 heterodimers and ZNT7 homodimers cooperatively play critical roles in TNAP activation by supplying zinc in human HAP1 cells, as in the case of chicken DT40 cells, although the effect produced by singly disrupting *ZNT5* or *ZNT7* in HAP1 cells appeared to differ slightly from that in DT40 cells.

ZNT5 uniquely recruits ZNT6 to Golgi apparatus by forming ZNT5–ZNT6 heterodimers

ZNT5 and ZNT6 have been widely demonstrated to form heterodimers and localize to the Golgi apparatus (47, 49, 50). However, the molecular features of ZNT5 and ZNT6 heterodimer formation have remained largely unknown thus far. ZNT6 expression levels were constant in HAP–*Z5Z7*-DKO cells regardless of the presence or absence of ZNT5 expression (Fig. 7*A*). Intriguingly, immunofluorescence staining revealed that ZNT6 was localized to the Golgi apparatus in WT HAP1 cells but not HAP–*Z5Z7*-DKO cells, and ZNT6 was thus found to be dispersed in the DKO cells (Fig. 7*B*, *1st* and *2nd columns*). Re-expression of ZNT5 in HAP–*Z5Z7*-DKO cells restored the Golgi localization of ZNT6 (Fig. 7*B*, *3rd column*) together with that of the re-expressed ZNT5 (Fig. 7*C*, *2nd column*). Moreover, this trafficking of ZNT6 to the Golgi by ZNT5 was found to be independent of the zinc transport activity of ZNT5, because the same effect was produced by the zinc transport–incompetent ZNT5$_{H451A}$ mutant (Fig. 7*C*, *3rd column*). We also confirmed that ZNT7 re-expression in HAP–*Z5Z7*-DKO cells did not affect ZNT6 localization; ZNT6 remained dispersed in the cells despite ZNT7 itself being localized to the Golgi apparatus (Fig. 7*B*, *4th column* and Fig. 7*D*). The dependence of ZNT6 localization on ZNT5 was also confirmed in HAP–*Z5*-KO cells (Fig. S4), where ZNT6 was dispersed in the cells, much as in HAP–*Z5Z7*-DKO cells. These results indicate that ZNT5 recruits ZNT6 to the Golgi apparatus to form the functional ZNT5–ZNT6 heterodimers that are required for activating zinc ectoenzymes such as TNAP.

Discussion

A fundamental but notable contribution of this study is that it clearly confirmed that the TNAP-activation functions of ZNT5–ZNT6 heterodimers and ZNT7 homodimers are highly conserved in eukaryotes, including plants. Specifically, our study revealed that human HAP1 cells lacking both of these ZNT complexes lost TNAP activity as in the case of chicken DT40 cells, and that this was reversed by the expression of human ZNTs and chicken ZNT orthologs in the cells. We previously showed that the reduced TNAP activity in TKO DT40 cells was reversed by both human ZNTs and chicken ZNT orthologs (24, 47), which indicated that the functions of ZNT

Figure 3. Conserved functions of Mtp12–Mtp5, plant ZNT5–ZNT6 orthologs, in Tnap activation. *A,* Mtp12 and Mtp5 or Mtp12 and svMtp5 form heterodimers. HA–Mtp12 and FLAG–Mtp5 or FLAG–svMtp5 were co-immunoprecipitated (*IP*) with antibodies against FLAG and HA tags, respectively, and 10% of each aliquot that was not subject to co-immunoprecipitation was immunoblotted (*input panel*). *B,* decreased Tnap activity in TKO cells was restored by co-expression of HA–Mtp12 and FLAG–Mtp5 but not HA–Mtp12 and FLAG–svMtp5. *C,* co-localization of Mtp12 and Mtp5 in the Golgi apparatus in DT40 cells stably expressing HA–Mtp12 and FLAG–Mtp5. FLAG–Mtp5 was also double-stained with GM130 (*right column*). *DAPI* staining and *merged* images are shown. *D,* replacement of histidine or aspartic acid with alanine in putative transmembranous zinc-binding site of Mtp12 (Mtp12$_{H452A}$ and Mtp12$_{D666A}$) led to a failure in the restoration of Tnap activity. *E,* restoration of Tnap activity by co-expression of untagged Mtp12 and Mtp5 was partial as compared with that following co-expression of ZNT5 and ZNT6 (ZNT5–ZNT6). *B* and *D*, stable expression of HA–Mtp12 or FLAG–Mtp5s was confirmed through immunoblotting. Cnx was used as the loading control. *B*, *D*, and *E*, measured Tnap activity is shown as means ± S.D. of triplicate experiments ($n = 3$). Statistical significance was analyzed by Student's *t* test in *B* and *E* or by one-way ANOVA followed by Tukey's post hoc test in *D*. **, $p < 0.01$. Each experiment was performed at least three times, and representative results from independent experiments are displayed.

Downloaded from http://www.jbc.org/ at Kyoto University on June 11, 2020

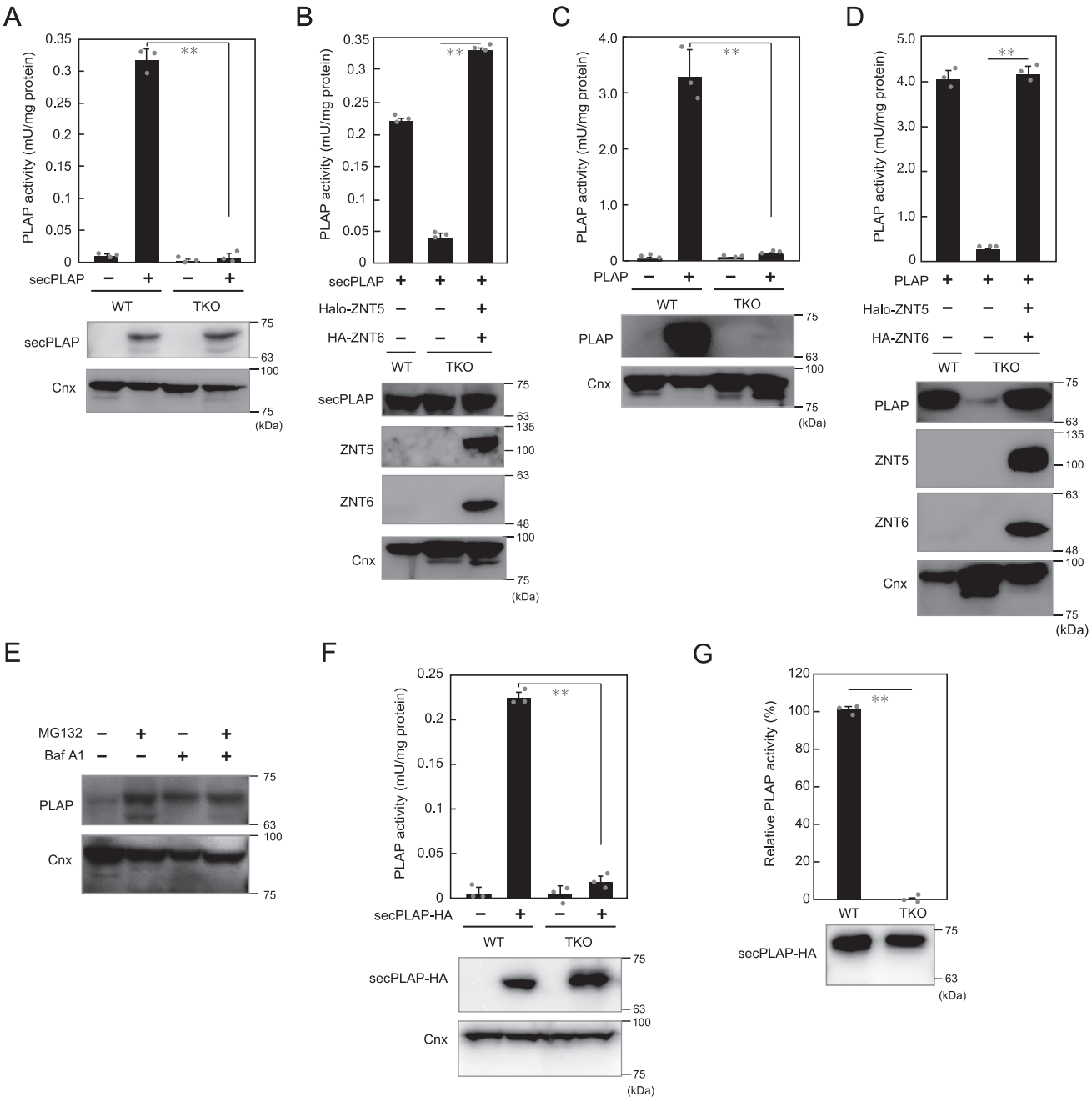

Downloaded from http://www.jbc.org/ at Kyoto University on June 11, 2020

complexes in the TNAP activation process are compatible between human and chicken. Intriguingly, however, TNAP activity exhibited certain differences when only one of the complexes was expressed in the cells: whereas TNAP activity was almost the same in WT HAP1 cells and HAP–*Z5*-KO or HAP–*Z7*-KO cells, Tnap activity relative to WT was decreased to 45–60% in *znt5*$^{-}$ DT40 cells and 20–30% in *znt7*$^{-/-}$ DT40 cells (24, 47). This phenomenon could be either species-specific or enzyme (TNAP)-specific, and to clarify this, it will be critical to characterize the properties of the respective ZNT complexes in humans and chickens from the viewpoint of the activity of each zinc ectoenzyme.

We have reported here a previously unrecognized unique property of ZNT5–ZNT6 heterodimers. The Golgi localization of ZNT6 observed in WT cells was lost in ZNT5-deficient cells (HAP–*Z5Z7*-DKO and HAP–*Z5*-KO cells), and this was restored following ZNT5 expression. Considering that ZNT6 localizes to the Golgi apparatus in WT HAP1 cells, in which ZNT6 forms heterodimers with ZNT5, the mechanism by which ZNT5 recruits ZNT6 to the Golgi apparatus is probably involved in the general regulation of ZNT5–ZNT6 heterodimer formation; this makes it likely that ZNT5–ZNT6 heterodimers supply zinc to zinc ectoenzymes such as TNAP and PLAP in or around the Golgi apparatus. How might ZNT5–ZNT6 heterodimers localize to the Golgi apparatus? One possibility is anterograde trafficking from the ER to the Golgi after heterodimerization in the ER, whereas another possibility is retrograde trafficking from cytosolic vesicles, where ZNT6 is localized as a protomer, to the Golgi apparatus after heterodimerization in the vesicles. We have not yet determined the precise subcellular localization of the ZNT6 protomer in HAP–*Z5Z7*-DKO and HAP–*Z5*-KO, and thus we cannot currently discriminate between these two possibilities. If ZNT5–ZNT6 heterodimer formation is also spatially controlled in other vertebrates, this might represent one of the reasons why most vertebrates harbor two ZNT complexes for mobilizing zinc into the lumen of the compartments of the early secretory pathway: the availability of distinct regulatory mechanisms for controlling the expression of ZNT5–ZNT6 heterodimers and ZNT7 homodimers could enable fine-tuning of zinc ectoenzyme activation. The genomes of certain eukaryotes code for only one of the ZNT transport complexes; for example, *Saccharomyces cerevisiae*, *Schizosaccharomyces pombe*, and *C. elegans* express only the ZNT5–ZNT6 ortholog (51–54), whereas *Drosophila melanogaster* expresses only the ZNT7 ortholog (40, 55–57). In such cases, other ZNT proteins might provide another zinc-entry route in the early secretory pathway and thus allow the fine-tuning of enzyme activation; however, our previous study excluded this possibility in the case of vertebrates: overexpression of ZNT1, ZNT2, ZNT3, ZNT4, and ZNT8 failed to activate TNAP (25). A recent study in *S. pombe* supports the aforementioned possibility, because Zhf1 (a distant ZNT homolog) in the ER plays a role in activating yeast ALP Pho8 redundantly with the Cis4–Zrg17 (ZNT5–ZNT6 ortholog) pathway in the Golgi apparatus (58, 59). Redundant zinc-entry routes in the early secretory pathway that are regulated in distinct manners would be necessary for appropriately activating numerous zinc-requiring protein functions during the life of an organism.

Another critical finding of this study is that relative to the ZNT transport complexes, ZIP9, ZIP13, and ZIP7 are unlikely to contribute substantially to the regulation of zinc ectoenzyme activation. This was also our speculation in previous studies (25, 33), but we clearly confirmed this here by using genetically-engineered cells. Tnap activity in TKO cells and TKO*zip9*$^{-/-}$*zip13*$^{-/-}$ cells was extremely low as compared with that in TKO*zip9*$^{-/-}$*zip13*$^{-/-}$ cells re-expressing ZNT5–ZNT6 heterodimers or ZNT7 homodimers (Fig. 2*C*). Given that ZIPs localized to the early secretory pathway have recently been widely reported to play crucial roles in the homeostasis of the early secretory pathway (29, 30, 32–34), our results suggest that ZNT5–ZNT6 heterodimers and ZNT7 homodimers directly and specifically manage the zinc supply to the target ectoenzymes independently of ZIPs.

We found that secPLAP–HA protein expressed in TKO cells was not detectable in either ALP zymography or immunoblotting performed using native-polyacrylamide gels, which could be because of the failure of secPLAP–HA to enter the native-polyacrylamide gels. Although the underlying reason remains to be determined, protein misfolding due to the loss of zinc metalation could be responsible. This might also explain why PLAP expressed in TKO cells was degraded through the cellular degradation pathway: the protein would have been misfolded because of impaired zinc metalation. Considering the differences between PLAP and secPLAP, the addition of the GPI anchor might facilitate the protein degradation, and addressing this question could provide information regarding the manner in which ZNT5–ZNT6 heterodimers and ZNT7 homodimers contribute to homeostatic maintenance in the early secretory pathway (48, 51). However, other possibilities also exist, such as homeostatic maintenance being achieved through the regulation of chaperone–protein functions by zinc that is mediated by both complexes (60, 61). Disruption of *Znt* and/or *Zip* genes in DT40 cells and *ZNT* genes in HAP1 cells increased the mRNA expression of other *Znt* and/or *Zip* genes in DT40 cells and *ZNT* genes in HAP1 cells (Figs. 1*A* and 2*A* and Fig. S3*A*). These

Figure 4. Lack of proper zinc metalation of secPLAP expressed in TKO cells. *A,* secPLAP activity was markedly decreased, but the protein was present in TKO cells. *B,* secPLAP activity in TKO cells was restored following the expression of ZNT5–ZNT6 heterodimers. *C,* PLAP activity was drastically decreased in TKO cells in conjunction with a loss of PLAP protein. *D,* PLAP activity and protein expression in TKO cells were restored following the expression of ZNT5–ZNT6 heterodimers. ZNT5 used in *B* and *D* was N-terminally fused with Halo-tag. *E,* PLAP protein expression was restored following treatment with inhibitors of lysosomal (bafilomycin A1 (*Baf A1*)) and proteasomal (MG132) degradation pathways. *F,* secPLAP–HA activity was markedly decreased, but the protein was present in TKO cells. *G,* relative activity of purified secPLAP–HA. *Lower panel,* immunoblot showing the contents of purified secPLAP–HA protein used to measure activity. *H,* relative zinc content was substantially decreased in secPLAP–HA purified from TKO cells as compared with that from WT cells. *I,* ALP zymography (*left*) and immunoblotting with native-PAGE (*right*) failed to reveal the activity and protein of secPLAP–HA purified from TKO cells. PLAP or secPLAP activity in all panels is expressed as means ± S.D. of triplicate experiments ($n = 3$). Statistical significance was analyzed by Student's *t* test in *A–D* and *F–H*. **, $p < 0.01$. Each experiment was performed at least three times, and representative results from independent experiments are shown.

Downloaded from http://www.jbc.org/ at Kyoto University on June 11, 2020

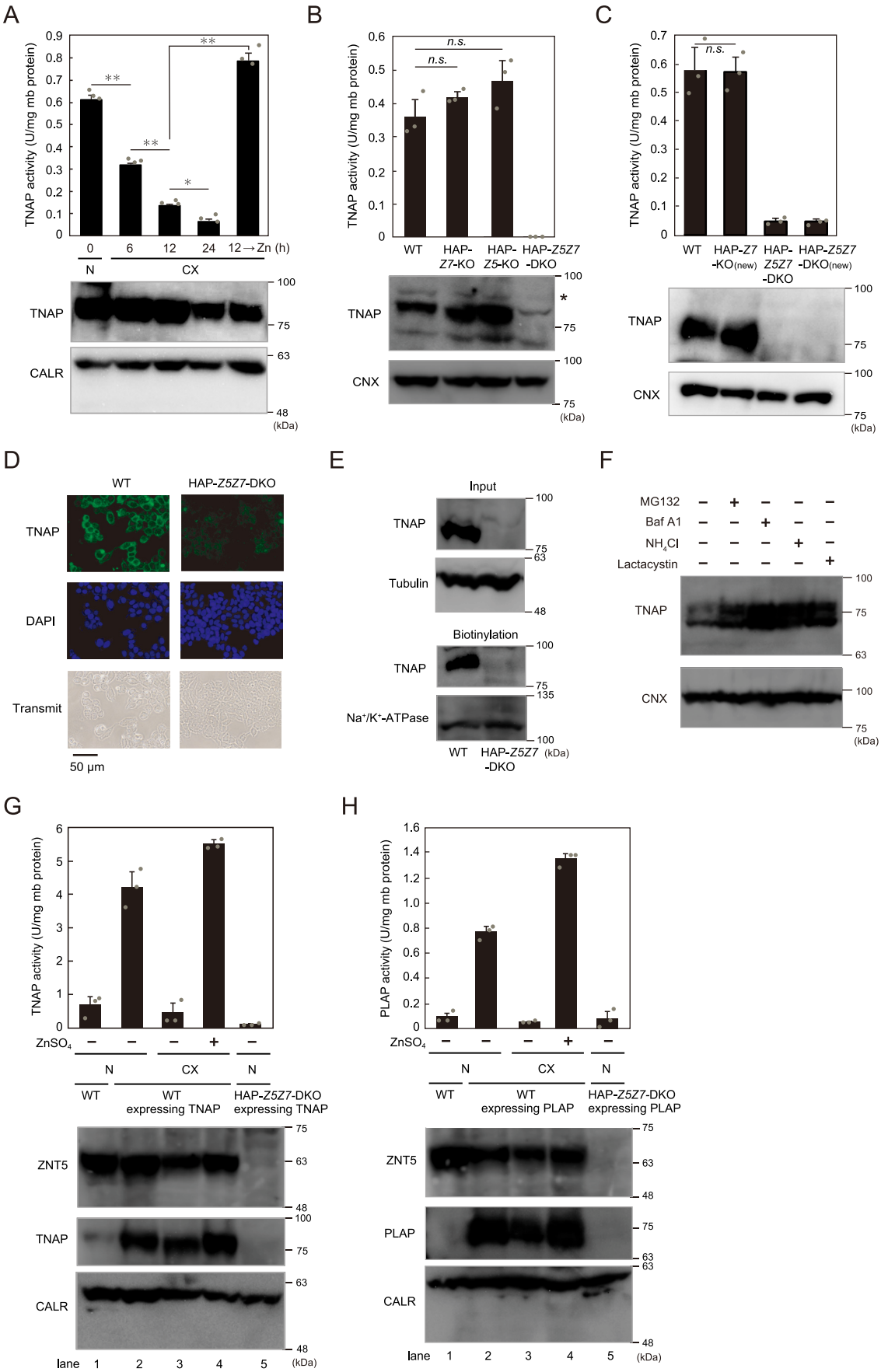

Downloaded from http://www.jbc.org/ at Kyoto University on June 11, 2020

results suggest that complex complementation mechanisms might act on the numerous zinc transporter proteins expressed in the early secretory pathway in vertebrate cells. As discussed above, the molecular mechanisms underlying these responses warrant further investigation.

Our results here provide insights into the molecular mechanism by which zinc ectoenzymes such as TNAP and PLAP are activated, revealing clearly that ZNT5–ZNT6 heterodimers and ZNT7 homodimers are indispensable for the activation process. However, our findings also raise several specific questions regarding the relationships between the "activity" and the "stability/degradation" of zinc ectoenzymes mediated by ZNT complexes. Why is it that secPLAP, the "GPI-deficient form," was not degraded in cells (Fig. 4*G*) but PLAP was? Why was PLAP expressed in DT40 TKO cells degraded more markedly (Fig. 4*C*) than PLAP expressed in *znt5*$^{-}$*znt7*$^{-/-}$ cells (24)? Why was TNAP not stabilized in HAP–*Z5Z7*-DKO cells stably expressing the zinc transport–incompetent $ZNT5_{H451A}$ mutant (Fig. 6*E*) but was stabilized in DT40 TKO cells stably expressing the mutant (25)? In relation to this last question, why was TNAP not completely degraded in WT HAP1 cells cultured under zinc-deficient conditions (Fig. 5*A*)? Answers to these questions will further enhance our understanding of the activation process of zinc ectoenzymes in the early secretory pathway. Novel approaches, including zinc-ome analysis, from a viewpoint of the relationships between "activity" and "stability/degradation" might be crucial for obtaining answers to these questions in future studies (62).

In conclusion, we addressed certain unresolved questions regarding the activation of zinc ectoenzymes by ZNT5–ZNT6 heterodimers and ZNT7 homodimers. 1) We found that ZIPs make minor contributions to TNAP activation. 2) We demonstrated that zinc metalation of PLAP produced in cells lacking both of the aforementioned ZNT complexes is impaired. 3) We confirmed that the function of the ZNT transport complexes in TNAP activation is highly conserved among eukaryotes. Furthermore, we uncovered a previously unknown unique mechanism regulating ZNT5–ZNT6 heterodimer formation, where ZNT5 recruits ZNT6 to the Golgi apparatus to form the heterodimers. As noted above, our results raise additional questions about the enzyme activation process; however, our findings also considerably enhance the current understanding of the process by providing new molecular insights into how zinc ectoenzymes are activated by zinc in the compartments of the early secretory pathway.

Experimental procedures

Plasmid construction

Plasmids for expressing epitope-tagged human ZIP13, ZIP9, and ZIP7 (both WT and mutants) were constructed by inserting each cDNA into the pA-Puro, pA-Zeocin, pA-Ecogpt, or pA-Neo vector (33, 37). The expression vectors for *Arabidopsis thaliana* Mtp12 and Mtp5 were constructed by inserting each cDNA into the pA-Puro or pA-Ecogpt vector. The FLAG- or HA-tag sequence was fused to respective genes by using a two-step PCR method, and the amplified cDNAs were sequenced in both directions. Mutations in Mtp12 expression plasmids ($Mtp12_{H452A}$ and $Mtp12_{D666A}$) were also introduced using a two-step PCR method. The FLAG-, HA-, or Halo-tagged ZNT5 and/or ZNT7 expression vectors used were described previously (27, 49), as were the plasmids for expressing TNAP and PLAP (27, 48). To construct secPLAP–HA expression plasmid, the encoding cDNA (46) was inserted into pA-Puro vector. To disrupt chicken *zip13*, the *zip13* fragments were PCR-amplified using gene-specific primers by using KOD-FX polymerase (TOYOBO, Osaka, Japan) with DT40 genomic DNA as a template and were then used for the long or short arms. The long or short arms were subcloned downstream or upstream of the drug-selection marker cassettes that included the drug-resistant genes (*Bsr* or *HisD*) flanked by mutant loxP sites (Fig. S1*A*). All plasmids were linearized using appropriate restriction enzymes before electroporation or lipofection.

Cell culture

Chicken B lymphocyte–derived DT40 cells were maintained in RPMI 1640 medium (Nacalai Tesque, Kyoto, Japan) supplemented with 10% (v/v) heat-inactivated fetal calf serum (FCS; Sigma), 1% (v/v) chicken serum (Invitrogen), and 50 μM 2-mercaptoethanol (Sigma) at 39.5 °C, as described previously (63). Human myelogenous leukemia HAP1 cells (purchased from Horizon Discovery, Cambridge, UK) were maintained in Iscove's modified Dulbecco's medium (Nacalai Tesque) containing 10% (v/v) heat-inactivated FCS (Sigma) at 37 °C. In certain experiments, to inhibit protein degradation, DT40 mutant cells were treated for 4 h with 100 μM MG132 (Peptide Institute, Osaka, Japan) or 100 nM bafilomycin A1 (Sigma) before collecting cells, or HAP1 mutant cells were cultured for 12 h in the presence of 10 μM MG132, 10 nM bafilomycin A1, 20 mM NH_4Cl, and 10 μM lactacystin (Peptide Institute, Osaka, Japan) before collect-

Figure 5. Concurrent disruption of *ZNT5* and *ZNT7* is required for decreasing TNAP activity in human HAP1 cells. *A,* TNAP activity was markedly decreased in HAP1 cells cultured in zinc-deficient medium (*CX*) for the indicated periods, but the reduced activity in CX medium for 12 h was restored by supplementing the medium with 20 μM $ZnSO_4$ for 12 h. *N*, normal culture. *B,* TNAP activity was decreased in HAP1 cells deficient in both *ZNT5* and *ZNT7* (HAP–*Z5Z7*–DKO cells) but not *ZNT5* or *ZNT7* alone (HAP–*Z5*–KO and HAP–*Z7*–KO cells). *, nonspecific band. *C,* same results as in *B* were obtained with a different set of KO cells: HAP–*Z7*–$KO_{(new)}$ and HAP–*Z5Z7*–$DKO_{(new)}$ cells. *A–C*, TNAP activity was measured using membrane proteins (*mb protein*) and is expressed as means ± S.D. of triplicate experiments. Calreticulin (CALR) and CNX are shown as loading controls. *D* and *E,* loss of TNAP cell-surface localization in HAP–*Z5Z7*–DKO cells. WT HAP1 and HAP–*Z5Z7*–DKO cells were subject to immunofluorescence staining (*D*) and cell-surface biotinylation assays (*E*). *D*, DAPI staining and transmitted light images are also shown. *E*, input refers to aliquots of the biotinylated proteins before avidin capture, and biotinylation refers to avidin-captured proteins; tubulin and Na^+/K^+-ATPase: loading controls for input and biotinylation, respectively. *F,* inhibition of lysosomal (bafilomycin A1 (*Baf A1*) or NH_4Cl) and proteasomal (MG132 or lactacystin) degradation pathways partially restored TNAP protein in HAP–*Z5Z7*–DKO cells. *G* and *H,* impairment of activation of TNAP and PLAP overexpressed in HAP–*Z5Z7*–DKO cells. *CALR:* loading control. *G*, total TNAP activity (exogenous plus endogenous TNAP activity) is shown. TNAP and PLAP activities are expressed as means ± S.D. of triplicate experiments ($n = 3$). Statistical significance was analyzed by one-way ANOVA followed by Tukey's post hoc test in *A* and *B* or by Student's *t* test in *C*. *, $p < 0.05$; **, $p < 0.01$; *n.s.*, not significant. Each experiment was performed at least three times, and representative results from independent experiments are displayed.

Downloaded from http://www.jbc.org/ at Kyoto University on June 11, 2020

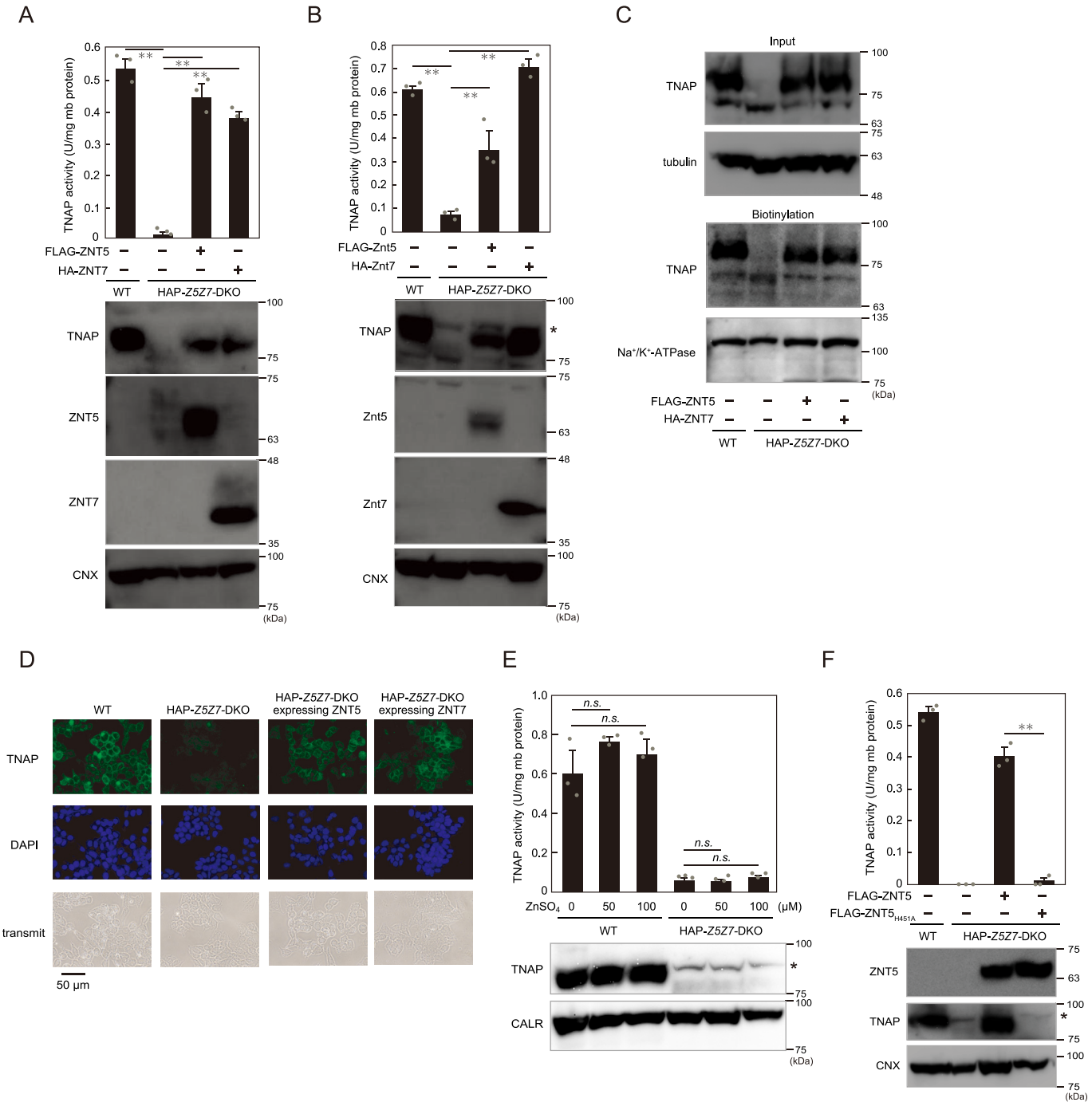

Figure 6. Reduced TNAP activity in HAP–*Z5Z7*–DKO cells is restored by ZNT5 or ZNT7 re-expression. *A*, restoration of TNAP activity in HAP–*Z5Z7*–DKO cells by re-expression of ZNT5 or ZNT7. *B*, TNAP activity in HAP–*Z5Z7*–DKO cells was also restored by re-expression of chicken Znt5 or Znt7 ortholog. *, nonspecific band. *C* and *D*, TNAP cell-surface localization following re-expression of ZNT5 or ZNT7 was confirmed in cell-surface biotinylation assays (*C*) and immunofluorescence staining (*D*) as described in Fig. 5, *D* and *E*. *E*, zinc supplementation for 24 h did not restore TNAP activity in HAP–*Z5Z7*–DKO cells. *, nonspecific band. *F*, expression of zinc transport–incompetent $ZNT5_{H451A}$ mutant failed to restore TNAP activity in HAP–*Z5Z7*–DKO cells. *, nonspecific band. *A*, *B*, *E*, and *F*, measured TNAP activity is shown as in Fig. 5 and is expressed as means ± S.D. of triplicate experiments ($n = 3$). Statistical significance was analyzed by one-way ANOVA followed by Tukey's post hoc test in *A*, *B*, and *E*, or by Student's *t* test in *F*. **, $p < 0.01$; *n.s.*, not significant. *CALR* and *CNX*: loading controls; *mb protein*, membrane protein. Each experiment was performed at least three times, and representative results from independent experiments are presented.

ing cells. To generate zinc-deficient culture medium, FCS or chicken serum was treated with Chelex-100 resin (Bio-Rad) as described (64). For zinc-supplementation experiments, cell-culture medium containing the indicated concentrations of $ZnSO_4$ was added.

Disruption of zip13 and/or zip9 in WT, zip9$^{-/-}$, and TKO DT40 cells

WT or *zip9*$^{-/-}$ cells were transfected sequentially with *zip13*-targeting vectors (Fig. S1*A*) by electroporation to disrupt *zip13*. To establish TKO*zip9*$^{-/-}$*zip13*$^{-/-}$ cells, TKO cells were

Downloaded from http://www.jbc.org/ at Kyoto University on June 11, 2020

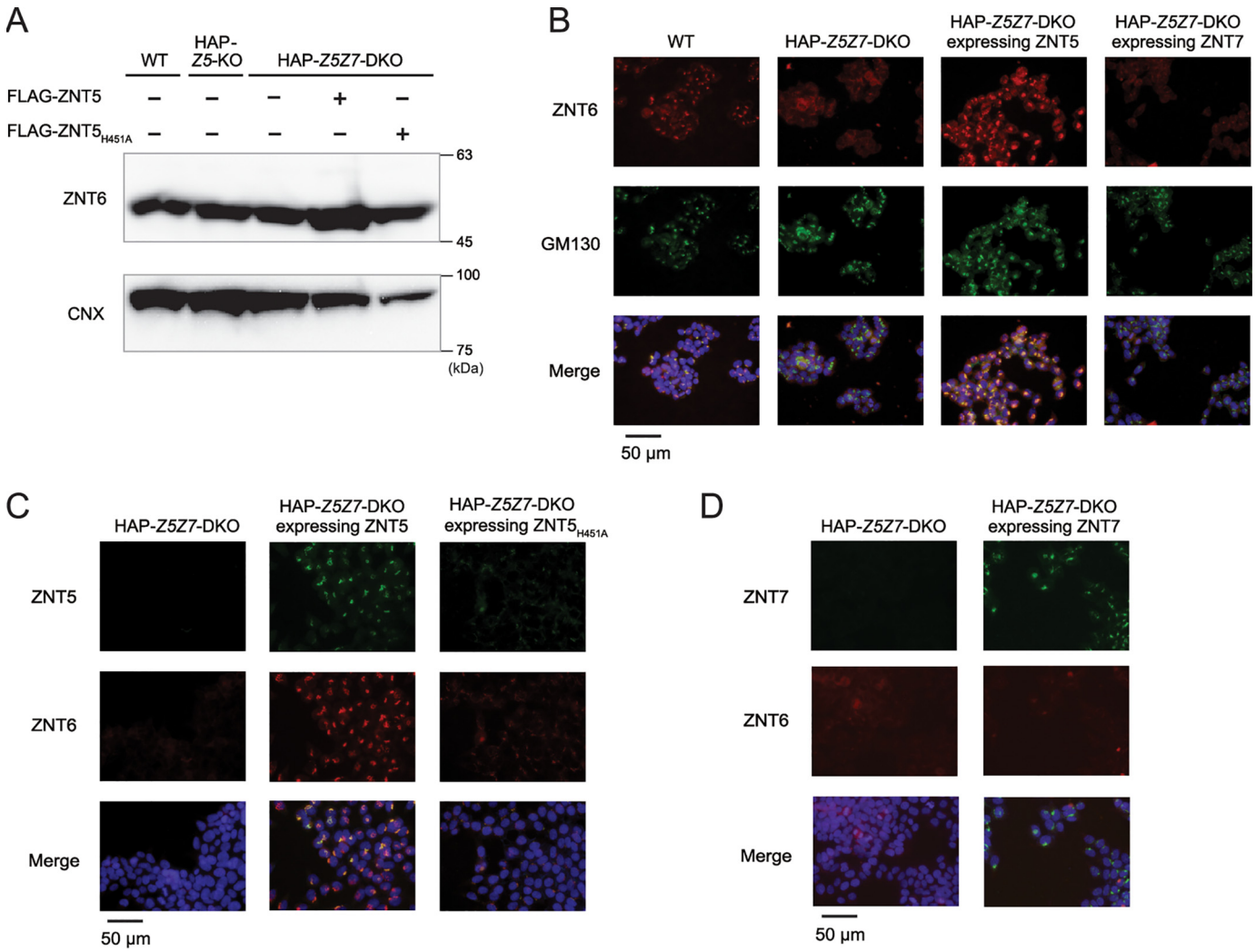

Figure 7. ZNT5 recruits ZNT6 to Golgi apparatus. *A,* ZNT6 expression was similar in WT, HAP–*Z5*–KO, HAP–*Z5Z7*–DKO, and HAP–*Z5Z7*–DKO cells stably expressing WT ZNT5 or $ZNT5_{H451A}$. Endogenous ZNT6 was detected with anti-ZNT6 antibody. *CNX,* loading control. *B–D,* ZNT6 localization to the Golgi apparatus depends on the expression of ZNT5 but not ZNT7. ZNT6 was co-stained with GM130 (*B*), ZNT5 (*C*), or ZNT7 (*D*) in the indicated cells. *Merged images* with DAPI staining are also shown. Each experiment was performed at least three times, and representative results from independent experiments are shown.

transfected sequentially with *zip9*- and *zip13*-targeting vectors after excising the drug-selection marker cassettes by using 4-hydroxytamoxifen (Sigma) as described previously (63). Gene disruption was confirmed by means of genomic DNA PCR or RT-PCR. Genomic DNA, which was prepared as described (63), was used as a template and PCR-amplified using KOD-FX (TOYOBO). The primers used for confirming *zip13* disruption (Fig. S1*A*) are listed in Table S1. RT-PCR was performed using total RNA isolated from harvested cells by using Sepasol I (Nacalai Tesque) and reverse-transcribed using ReverTra Ace (TOYOBO). PCR was performed using KOD-FX. The primers used in RT-PCR are listed in Table S2. Electroporation was used to establish DT40 disruptants.

Disruption of ZNT5 and/or ZNT7 in HAP1 cells

ZNT5 and/or *ZNT7* gene disruption was performed through CRISPR/Cas9-mediated genome editing (Table 1). Oligonucleotides for generating sgRNA expression plasmids were annealed and cloned into the BbsI or BsaI site of PX-330-B/B vector (3). The following oligonucleotides were used: *ZNT7–152F,* 5′-CACCTGGAACTACTCTACGGCATC-3′; *ZNT7–152R,* 5′-AAACGATGCCGTAGAGTAGTTCCA-3′; *ZNT5*-1510F, 5′-CACCGGCGTGCTGACCAATAGTCT-3′; and *ZNT5*-1510R, 5′-AAACAGACTATTGGTCAGCACGCC-3′ (guide RNA sequences are underlined). The constructed plasmids and one-tenth quantity of pcDNA6/TR (containing blasticidin S-resistance gene) or pA-puro (containing puromycin-resistance gene) were co-transfected into 80% confluent HAP1 cells by using Lipofectamine 2000 (Invitrogen). The cells were cultured for 1 day and transferred to a 10-cm cell culture dish and treated with 20 μg/ml blasticidin (InvivoGen, San Diego, CA) or 0.75 μg/ml puromycin (Sigma) to establish stable clones. HAP1 cells deficient in *ZNT5* and/or *ZNT7* were confirmed by directly sequencing the fragments amplified using genomic-DNA PCR and RT-PCR; the primers used are shown in Table S3. *ZNT7*-KO HAP1 (HAP–*Z7*-KO) cells were purchased from Horizon Discovery.

Measurement of ALP activity

Membrane proteins or total-protein extracts from cells were prepared in ALP lysis buffer, and 3 or 5 μg of membrane proteins or 5 μg of total proteins were used for measuring TNAP or PLAP activity, as described previously (63). For measuring the

Downloaded from http://www.jbc.org/ at Kyoto University on June 11, 2020

Table 1
Mutations introduced in *ZNT5* and/or *ZNT7* in HAP1 cells used in this study

Cells	Targeted region	Mutation
HAP–*Z5*-KO[a]	Exon 11	1-bp insertion in *ZNT5*
HAP–*Z7*-KO[a]	Exon 2	28-bp deletion in *ZNT7*
HAP–*Z5Z7*-DKO[a]	Exon 11 in *ZNT5*, exon 2 in *ZNT7*	2-bp deletion in *ZNT5* and 28-bp deletion in *ZNT7*
HAP–*Z7*-$KO_{(new)}$	Exon 2	165-bp insertion
HAP–*Z5Z7*-$DKO_{(new)}$[a]	Exon 11 in *ZNT5*, exon 2 in *ZNT7*	32-bp deletion in *ZNT5*, 165-bp insertion in *ZNT7*

[a] The detailed investigation is shown in Fig. S3.

activity of purified secPLAP–HA, we used the same amounts of protein estimated from SDS-PAGE band intensity. The released *p*-nitrophenol was quantified by measuring the 405-nm absorbance of assay samples. PLAP activity was measured after samples were treated at 65 °C for 30 min.

Immunoblotting

Immunoblotting was performed as described previously (65). Briefly, blotted polyvinylidene difluoride membranes (Immobilon-P, Millipore Corp., Bedford, MA) were blocked with 5% skimmed milk, 0.1% Tween 20 in PBS and then incubated with primary antibodies (diluted in blocking buffer): anti-FLAG M2 (1:3000; F3165, Sigma); anti-HA-11 (1:3000; MMS-101P, Covance, Emeryville, CA); anti-HA clone 3F10 (1:3000; 11867423001, Roche Applied Science, Mannheim, Baden-Württemberg, Germany); anti-Myc (1:3000; sc-40, Santa Cruz Biotechnology Inc., Santa Cruz, CA); anti-TNAP (1:3000; sc-30203 and sc-166261, Santa Cruz Biotechnology); anti-PLAP (1:3000; sc-15065 (L-19), or sc-47691, Santa Cruz Biotechnology); anti-calnexin (1:6000; ADI-SPA-860, Enzo Life Sciences, Plymouth Meeting, PA); anti-calreticulin (1:5000; PA3–900, Affinity Bioreagents, Golden, CO); anti-ZNT5 (1:1000) (17); anti-ZNT6 (1:3000; 13526–1-AP, Proteintech Group Inc., Chicago, IL); or anti-α-tubulin (1:5000; 12G10, deposited to Developmental Studies Hybridoma Bank by J. Frankel and E. M. Nelsen). Immunoreactive bands were detected using 1:3000 horseradish peroxidase–conjugated anti-mouse or anti-rabbit secondary antibodies (NA931 or NA934, GE Healthcare) or anti-goat secondary antibody (sc-2020, Santa Cruz Biotechnology) and Immobilon Western Chemiluminescent HRP substrates (Millipore) or SuperSignal West Femto Maximum Sensitivity substrate (Pierce). Fluoro-images were obtained using an LAS 500 (GE Healthcare).

Cell-surface biotinylation assay

Cell-surface biotinylation assay was performed, as described previously (65). After washing cells with PBS, we added EZ-Link, a sulfo-NHS–SS–biotin reagent (Pierce Protein Biology , Thermo Fisher Scientific). Subsequently, biotinylated proteins were captured using streptavidin-coupled beads and recovered in 6× SDS sample buffer and immunoblotted.

Co-immunoprecipitation

Co-immunoprecipitation was performed, as described previously (24). Briefly, 200 μg of membrane proteins were prepared from DT40 cells stably expressing HA–Mtp12 and FLAG–Mtp5s after lysis in an NP-40 buffer containing 0.05% SDS, and proteins were then immunoprecipitated with the following monoclonal antibodies: anti-FLAG M2 (1:200) and anti-HA (1:200; HA11). After rotating samples for 1 h, 15 μl of protein G–Sepharose beads (GE Healthcare) were added, and the sample tubes were rotated again (overnight, at 4 °C). Subsequently, the samples were centrifuged at 15,000 rpm for 5 min, and the pelleted beads containing the immunoprecipitates were washed three times with the NP-40 buffer without SDS and eluted with 12.5 μl of 2× urea buffer and 2.5 μl of Ling's solubilizing buffer. After incubation for 30 min at room temperature, 13 μl of each supernatant was electrophoresed; 20 μg of membrane proteins that were not subject to co-immunoprecipitation were used as the input fraction. Immunoreactive bands were detected as described above.

Immunofluorescence staining

Immunostaining was performed, as described previously (24, 63), with these first antibodies: anti-FLAG (1:2000; anti-DDDDK; MBL, Nagoya, Japan); anti-HA (1:1000; HA11) and anti-GM130 (1:1000; 610823, BD Transduction Laboratories); anti-ZNT5 (1:500) and anti-ZNT6 (1:500; HPA055032; Atlas Antibodies AB, Stockholm, Sweden), or anti-TNAP (1:500). The second and third antibodies used were Alexa 488–conjugated goat anti-rabbit IgG, rabbit anti-goat IgG, and goat anti-mouse IgG, and Alexa 594–conjugated donkey anti-rabbit IgG (all from Molecular Probes, Eugene, OR). The antibodies were applied at room temperature for 1 h or at 4 °C overnight, and 4,6-diamino-2-phenylindole (DAPI) was added during second and third antibody staining to label nuclei. For staining TNAP, the second and third antibodies were diluted, respectively, with Can Get Signal Solution B and Can Get Signal Solution A (TOYOBO); otherwise, 2% BSA in PBS was used as the dilution buffer. The stained cells were examined using a fluorescence microscope (FSX100; Olympus, Tokyo, Japan), and images were analyzed using Adobe Photoshop CS. Identical exposure settings and times were used for the corresponding images in each figure.

Purification of secPLAP–HA

DT40 WT or TKO cells stably expressing secPLAP–HA were collected and resuspended in 5 ml of cold homogenizing buffer (0.25 M sucrose, 20 mM HEPES, 1 mM EDTA). After homogenization (30 strokes, 10×) in a 7-ml Dounce homogenizer on ice, homogenates were centrifuged at 2300 × *g* for 5 min at 4 °C, and the obtained post-nuclear supernatant was centrifuged at 15,000 × *g* for 30 min at 4 °C. The supernatant was collected as sup A. The pellet was lysed in lysis buffer (0.1% NP-40, 50 mM HEPES, 100 mM NaCl, 1.5 mM $MgCl_2$), and the lysate was centrifuged at 10,000 × *g* for 5 min at 4 °C to remove insoluble fractions. The supernatant was collected as sup B. The secPLAP–HA in the mixture of sup A and sup B was recovered through incubation (with

Downloaded from http://www.jbc.org/ at Kyoto University on June 11, 2020

rotation) with anti-HA antibody magnetic beads (MBL) for 16 h at 4 °C. The beads containing secPLAP–HA protein were washed three times each with PBS/Tween 20 and PBS, and the proteins were eluted using PBS containing 1 mg/ml HA peptide (MBL). To determine relative concentrations, proteins were silver-stained using a Silver Stain MS kit (Wako Pure Chemicals, Osaka, Japan) after SDS-PAGE, and the captured images were analyzed using ImageQuant TL (GE Healthcare).

ICP-MS

Purified secPLAP–HA was decomposed with 1.0 ml of nitric acid under microwave heating, and the sample solutions were then evaporated to dryness on a hot plate and re-dissolved in 1% nitric acid for elemental analysis by using ICP-MS. The signal intensity of zinc was monitored at m/z 68, with an integration time of 0.1 s. The zinc content measurements obtained were normalized against protein content.

Native-PAGE and ALP zymography

Purified secPLAP–HA was separated through native-PAGE by using gradient gels (Invitrogen) with 4× native-PAGE sample buffer (40% glycerol, 0.4% bromphenol blue, 200 mM Tris-HCl, pH 6.8). To perform ALP zymography, gels were rinsed in TBS buffer for 10 min and then stained with a BCIP-NBP solution kit (Nacalai Tesque) to visualize ALP activity.

Statistical analyses

All data are expressed as the mean ± S.D. of triplicate experiments. Statistical significance was determined by the one-way analysis of variance (ANOVA) followed by Tukey's post hoc test (comparison for three or more groups) or Student's t test (comparison for two groups) at $p < 0.05$ (*) and $p < 0.01$ (**).

Data availability

All data generated or analyzed during this study are included in this published article (and its supporting information) or are available from the corresponding author (Taiho Kambe, Kyoto University) upon reasonable request.

Author contributions—E. S., N. O., T.-a. T., Y. N., Y.-k. T., T. F., M. M., S. U., N. K., T. T., Y. O., and T. K. data curation; E. S., N. O., T.-a. T., Y. N., Y.-k. T., T. F., Y. O., and T. K. software; E. S., N. O., T.-a. T., Y. N., Y.-k. T., T. F., M. M., S. U., N. K., T. T., Y. O., and T. K. formal analysis; E. S., N. O., T.-a. T., Y. N., Y.-k. T., T. F., M. M., S. U., N. K., and T. K. validation; E. S., N. O., T.-a. T., Y. N., T. F., M. M., S. U., N. K., T. T., A. F., T. Y., and T. K. investigation; E. S., N. O., T.-a. T., Y. N., and T. K. visualization; E. S., N. O., T.-a. T., Y. N., Y.-k. T., Y. O., and T. K. methodology; T. T., A. F., T. Y., K. M. T., Y. O., and T. K. writing-review and editing; A. F., T. Y., K. M. T., and T. K. resources; T. K. conceptualization; T. K. supervision; Y. O. and T. K. funding acquisition; T. K. writing-original draft; T. K. project administration.

Acknowledgments—We thank Dr. Andrew Stoker (UCL Institute of Child Health) for the PLAP–HA plasmid (secPLAP–HA in this study), and Dr. Naoya Itsumura and Kazuhisa Fukue for experimental suggestions and support. We also thank Shuangyu Luo, Tsukihi Naruse, and Momoko Yamamoto for helpful technical assistance.

References

1. Palmiter, R. D., and Findley, S. D. (1995) Cloning and functional characterization of a mammalian zinc transporter that confers resistance to zinc. *EMBO J.* **14,** 639–649 CrossRef Medline
2. Leyva-Illades, D., Chen, P., Zogzas, C. E., Hutchens, S., Mercado, J. M., Swaim, C. D., Morrisett, R. A., Bowman, A. B., Aschner, M., and Mukhopadhyay, S. (2014) SLC30A10 is a cell surface-localized manganese efflux transporter, and parkinsonism-causing mutations block its intracellular trafficking and efflux activity. *J. Neurosci.* **34,** 14079–14095 CrossRef Medline
3. Nishito, Y., and Kambe, T. (2019) Zinc transporter 1 (ZNT1) expression on the cell surface is elaborately controlled by cellular zinc levels. *J. Biol. Chem.* **294,** 15686–15697 CrossRef Medline
4. Lichten, L. A., and Cousins, R. J. (2009) Mammalian zinc transporters: nutritional and physiologic regulation. *Annu. Rev. Nutr.* **29,** 153–176 CrossRef Medline
5. Kambe, T. (2012) Molecular architecture and function of ZnT transporters. *Curr. Top. Membr.* **69,** 199–220 CrossRef Medline
6. Cole, T. B., Wenzel, H. J., Kafer, K. E., Schwartzkroin, P. A., and Palmiter, R. D. (1999) Elimination of zinc from synaptic vesicles in the intact mouse brain by disruption of the ZnT3 gene. *Proc. Natl. Acad. Sci. U.S.A.* **96,** 1716–1721 CrossRef Medline
7. Chowanadisai, W., Lönnerdal, B., and Kelleher, S. L. (2006) Identification of a mutation in SLC30A2 (ZnT-2) in women with low milk zinc concentration that results in transient neonatal zinc deficiency. *J. Biol. Chem.* **281,** 39699–39707 CrossRef Medline
8. Lemaire, K., Ravier, M. A., Schraenen, A., Creemers, J. W., Van de Plas, R., Granvik, M., Van Lommel, L., Waelkens, E., Chimienti, F., Rutter, G. A., Gilon, P., in't Veld, P. A., and Schuit, F. C. (2009) Insulin crystallization depends on zinc transporter ZnT8 expression, but is not required for normal glucose homeostasis in mice. *Proc. Natl. Acad. Sci. U.S.A.* **106,** 14872–14877 CrossRef Medline
9. Sindreu, C., Palmiter, R. D., and Storm, D. R. (2011) Zinc transporter ZnT-3 regulates presynaptic Erk1/2 signaling and hippocampus-dependent memory. *Proc. Natl. Acad. Sci. U.S.A.* **108,** 3366–3370 CrossRef Medline
10. Podany, A. B., Wright, J., Lamendella, R., Soybel, D. I., and Kelleher, S. L. (2016) ZnT2-mediated zinc import into Paneth cell granules is necessary for coordinated secretion and Paneth cell function in mice. *Cell. Mol. Gastroenterol. Hepatol.* **2,** 369–383 CrossRef Medline
11. Kelleher, S. L., McCormick, N. H., Velasquez, V., and Lopez, V. (2011) Zinc in specialized secretory tissues: roles in the pancreas, prostate, and mammary gland. *Adv. Nutr.* **2,** 101–111 CrossRef Medline
12. Kambe, T. (2011) An overview of a wide range of functions of ZnT and Zip zinc transporters in the secretory pathway. *Biosci. Biotechnol. Biochem.* **75,** 1036–1043 CrossRef Medline
13. Hennigar, S. R., and Kelleher, S. L. (2012) Zinc networks: the cell-specific compartmentalization of zinc for specialized functions. *Biol. Chem.* **393,** 565–578 CrossRef Medline
14. Merriman, C., Huang, Q., Rutter, G. A., and Fu, D. (2016) Lipid-tuned zinc transport activity of human ZnT8 protein correlates with risk for type-2 diabetes. *J. Biol. Chem.* **291,** 26950–26957 CrossRef Medline
15. Huang, Q., Merriman, C., Zhang, H., and Fu, D. (2017) Coupling of insulin secretion and display of a granule-resident zinc transporter ZnT8 on the surface of pancreatic beta cells. *J. Biol. Chem.* **292,** 4034–4043 CrossRef Medline
16. Fukue, K., Itsumura, N., Tsuji, N., Nishino, K., Nagao, M., Narita, H., and Kambe, T. (2018) Evaluation of the roles of the cytosolic N terminus and His-rich loop of ZNT proteins using ZNT2 and ZNT3 chimeric mutants. *Sci. Rep.* **8,** 14084 CrossRef Medline
17. Kambe, T., Narita, H., Yamaguchi-Iwai, Y., Hirose, J., Amano, T., Sugiura, N., Sasaki, R., Mori, K., Iwanaga, T., and Nagao, M. (2002) Cloning and characterization of a novel mammalian zinc transporter, zinc transporter 5, abundantly expressed in pancreatic beta cells. *J. Biol. Chem.* **277,** 19049–19055 CrossRef Medline

Downloaded from http://www.jbc.org/ at Kyoto University on June 11, 2020

18. Huang, L., Kirschke, C. P., and Gitschier, J. (2002) Functional characterization of a novel mammalian zinc transporter, ZnT6. *J. Biol. Chem.* **277,** 26389–26395 CrossRef Medline
19. Kirschke, C. P., and Huang, L. (2003) ZnT7, a novel mammalian zinc transporter, accumulates zinc in the Golgi apparatus. *J. Biol. Chem.* **278,** 4096–4102 CrossRef Medline
20. Kambe, T., Takeda, T. A., and Nishito, Y. (2016) Activation of zinc-requiring ectoenzymes by ZnT transporters during the secretory process: biochemical and molecular aspects. *Arch. Biochem. Biophys.* **611,** 37–42 CrossRef Medline
21. Kambe, T., Matsunaga, M., and Takeda, T. A. (2017) Understanding the contribution of zinc transporters in the function of the early secretory pathway. *Int. J. Mol. Sci.* **18,** E2179 CrossRef Medline
22. Mornet, E., Stura, E., Lia-Baldini, A. S., Stigbrand, T., Ménez, A., and Le Du, M. H. (2001) Structural evidence for a functional role of human tissue nonspecific alkaline phosphatase in bone mineralization. *J. Biol. Chem.* **276,** 31171–31178 CrossRef Medline
23. Le Du, M. H., Stigbrand, T., Taussig, M. J., Menez, A., and Stura, E. A. (2001) Crystal structure of alkaline phosphatase from human placenta at 1.8 A resolution. Implication for a substrate specificity. *J. Biol. Chem.* **276,** 9158–9165 CrossRef Medline
24. Suzuki, T., Ishihara, K., Migaki, H., Matsuura, W., Kohda, A., Okumura, K., Nagao, M., Yamaguchi-Iwai, Y., and Kambe, T. (2005) Zinc transporters, ZnT5 and ZnT7, are required for the activation of alkaline phosphatases, zinc-requiring enzymes that are glycosylphosphatidylinositol-anchored to the cytoplasmic membrane. *J. Biol. Chem.* **280,** 637–643 CrossRef Medline
25. Fukunaka, A., Kurokawa, Y., Teranishi, F., Sekler, I., Oda, K., Ackland, M. L., Faundez, V., Hiromura, M., Masuda, S., Nagao, M., Enomoto, S., and Kambe, T. (2011) Tissue nonspecific alkaline phosphatase is activated via a two-step mechanism by zinc transport complexes in the early secretory pathway. *J. Biol. Chem.* **286,** 16363–16373 CrossRef Medline
26. Tsuji, T., Kurokawa, Y., Chiche, J., Pouysségur, J., Sato, H., Fukuzawa, H., Nagao, M., and Kambe, T. (2017) Dissecting the process of activation of cancer-promoting zinc-requiring ectoenzymes by zinc metalation mediated by ZNT transporters. *J. Biol. Chem.* **292,** 2159–2173 CrossRef Medline
27. Takeda, T. A., Miyazaki, S., Kobayashi, M., Nishino, K., Goto, T., Matsunaga, M., Ooi, M., Shirakawa, H., Tani, F., Kawamura, T., Komai, M., and Kambe, T. (2018) Zinc deficiency causes delayed ATP clearance and adenosine generation in rats and cell culture models. *Commun. Biol.* **1,** 113 CrossRef Medline
28. Jeong, J., Walker, J. M., Wang, F., Park, J. G., Palmer, A. E., Giunta, C., Rohrbach, M., Steinmann, B., and Eide, D. J. (2012) Promotion of vesicular zinc efflux by ZIP13 and its implications for spondylocheiro dysplastic Ehlers-Danlos syndrome. *Proc. Natl. Acad. Sci. U.S.A.* **109,** E3530–E3538 CrossRef Medline
29. Ohashi, W., Kimura, S., Iwanaga, T., Furusawa, Y., Irié, T., Izumi, H., Watanabe, T., Hijikata, A., Hara, T., Ohara, O., Koseki, H., Sato, T., Robine, S., Mori, H., Hattori, Y., *et al.* (2016) Zinc transporter SLC39A7/ZIP7 promotes intestinal epithelial self-renewal by resolving ER stress. *PLoS Genet.* **12,** e1006349 CrossRef Medline
30. Bin, B. H., Bhin, J., Seo, J., Kim, S. Y., Lee, E., Park, K., Choi, D. H., Takagishi, T., Hara, T., Hwang, D., Koseki, H., Asada, Y., Shimoda, S., Mishima, K., and Fukada, T. (2017) Requirement of zinc transporter SLC39A7/ZIP7 for dermal development to fine-tune endoplasmic reticulum function by regulating protein disulfide isomerase. *J. Invest. Dermatol.* **137,** 1682–1691 CrossRef Medline
31. Fauster, A., Rebsamen, M., Willmann, K. L., César-Razquin, A., Girardi, E., Bigenzahn, J. W., Schischlik, F., Scorzoni, S., Bruckner, M., Konecka, J., Hörmann, K., Heinz, L. X., Boztug, K., and Superti-Furga, G. (2019) Systematic genetic mapping of necroptosis identifies SLC39A7 as modulator of death receptor trafficking. *Cell Death Differ.* **26,** 1138–1155 CrossRef Medline
32. Tuncay, E., Bitirim, V. C., Durak, A., Carrat, G. R. J., Taylor, K. M., Rutter, G. A., and Turan, B. (2017) Hyperglycemia-induced changes in ZIP7 and ZnT7 expression cause Zn^{2+} release from the sarco(endo)plasmic reticulum and mediate ER stress in the heart. *Diabetes* **66,** 1346–1358 CrossRef Medline
33. Matsuura, W., Yamazaki, T., Yamaguchi-Iwai, Y., Masuda, S., Nagao, M., Andrews, G. K., and Kambe, T. (2009) SLC39A9 (ZIP9) regulates zinc homeostasis in the secretory pathway: characterization of the ZIP subfamily I protein in vertebrate cells. *Biosci. Biotechnol. Biochem.* **73,** 1142–1148 CrossRef Medline
34. Woodruff, G., Bouwkamp, C. G., de Vrij, F. M., Lovenberg, T., Bonaventure, P., Kushner, S. A., and Harrington, A. W. (2018) The zinc transporter SLC39A7 (ZIP7) is essential for regulation of cytosolic zinc levels. *Mol. Pharmacol.* **94,** 1092–1100 CrossRef Medline
35. Fukada, T., Civic, N., Furuichi, T., Shimoda, S., Mishima, K., Higashiyama, H., Idaira, Y., Asada, Y., Kitamura, H., Yamasaki, S., Hojyo, S., Nakayama, M., Ohara, O., Koseki, H., Dos Santos, H. G., *et al.* (2008) The zinc transporter SLC39A13/ZIP13 is required for connective tissue development; its involvement in BMP/TGF-β signaling pathways. *PLoS ONE* **3,** e3642 CrossRef Medline
36. Hogstrand, C., Kille, P., Nicholson, R. I., and Taylor, K. M. (2009) Zinc transporters and cancer: a potential role for ZIP7 as a hub for tyrosine kinase activation. *Trends Mol. Med.* **15,** 101–111 CrossRef Medline
37. Taylor, K. M., Hiscox, S., Nicholson, R. I., Hogstrand, C., and Kille, P. (2012) Protein kinase CK2 triggers cytosolic zinc signaling pathways by phosphorylation of zinc channel ZIP7. *Sci. Signal.* **5,** ra11 CrossRef Medline
38. Taniguchi, M., Fukunaka, A., Hagihara, M., Watanabe, K., Kamino, S., Kambe, T., Enomoto, S., and Hiromura, M. (2013) Essential role of the zinc transporter ZIP9/SLC39A9 in regulating the activations of Akt and Erk in B-cell receptor signaling pathway in DT40 Cells. *PLoS ONE* **8,** e58022 CrossRef Medline
39. Fujimoto, S., Tsuji, T., Fujiwara, T., Takeda, T. A., Merriman, C., Fukunaka, A., Nishito, Y., Fu, D., Hoch, E., Sekler, I., Fukue, K., Miyamae, Y., Masuda, S., Nagao, M., and Kambe, T. (2016) The PP-motif in luminal loop 2 of ZnT transporters plays a pivotal role in TNAP activation. *Biochem. J.* **473,** 2611–2621 CrossRef Medline
40. Kambe, T., Suzuki, T., Nagao, M., and Yamaguchi-Iwai, Y. (2006) Sequence similarity and functional relationship among eukaryotic ZIP and CDF transporters. *Genomics Proteomics Bioinformatics* **4,** 1–9 CrossRef Medline
41. Maret, W. (2011) Redox biochemistry of mammalian metallothioneins. *J. Biol. Inorg. Chem.* **16,** 1079–1086 CrossRef Medline
42. Kimura, T., and Kambe, T. (2016) The functions of metallothionein and ZIP and ZnT transporters: an overview and perspective. *Int. J. Mol. Sci.* **17,** 336 CrossRef Medline
43. Nimmanon, T., Ziliotto, S., Morris, S., Flanagan, L., and Taylor, K. M. (2017) Phosphorylation of zinc channel ZIP7 drives MAPK, PI3K and mTOR growth and proliferation signalling. *Metallomics* **9,** 471–481 CrossRef Medline
44. Fujiwara, T., Kawachi, M., Sato, Y., Mori, H., Kutsuna, N., Hasezawa, S., and Maeshima, M. (2015) A high molecular mass zinc transporter MTP12 forms a functional heteromeric complex with MTP5 in the Golgi in *Arabidopsis thaliana*. *FEBS J.* **282,** 1965–1979 CrossRef Medline
45. Berger, J., Hauber, J., Hauber, R., Geiger, R., and Cullen, B. R. (1988) Secreted placental alkaline phosphatase: a powerful new quantitative indicator of gene expression in eukaryotic cells. *Gene* **66,** 1–10 CrossRef Medline
46. Lee, S., Faux, C., Nixon, J., Alete, D., Chilton, J., Hawadle, M., and Stoker, A. W. (2007) Dimerization of protein tyrosine phosphatase sigma governs both ligand binding and isoform specificity. *Mol. Cell. Biol.* **27,** 1795–1808 CrossRef Medline
47. Suzuki, T., Ishihara, K., Migaki, H., Ishihara, K., Nagao, M., Yamaguchi-Iwai, Y., and Kambe, T. (2005) Two different zinc transport complexes of cation diffusion facilitator proteins localized in the secretory pathway operate to activate alkaline phosphatases in vertebrate cells. *J. Biol. Chem.* **280,** 30956–30962 CrossRef Medline
48. Ishihara, K., Yamazaki, T., Ishida, Y., Suzuki, T., Oda, K., Nagao, M., Yamaguchi-Iwai, Y., and Kambe, T. (2006) Zinc transport complexes contribute to the homeostatic maintenance of secretory pathway function in vertebrate cells. *J. Biol. Chem.* **281,** 17743–17750 CrossRef Medline

Downloaded from http://www.jbc.org/ at Kyoto University on June 11, 2020

49. Fukunaka, A., Suzuki, T., Kurokawa, Y., Yamazaki, T., Fujiwara, N., Ishihara, K., Migaki, H., Okumura, K., Masuda, S., Yamaguchi-Iwai, Y., Nagao, M., and Kambe, T. (2009) Demonstration and characterization of the heterodimerization of ZnT5 and ZnT6 in the early secretory pathway. *J. Biol. Chem.* **284,** 30798–30806 CrossRef Medline
50. Lasry, I., Golan, Y., Berman, B., Amram, N., Glaser, F., and Assaraf, Y. G. (2014) *In situ* dimerization of multiple wild type and mutant zinc transporters in live cells using bimolecular fluorescence complementation. *J. Biol. Chem.* **289,** 7275–7292 CrossRef Medline
51. Ellis, C. D., Wang, F., MacDiarmid, C. W., Clark, S., Lyons, T., and Eide, D. J. (2004) Zinc and the Msc2 zinc transporter protein are required for endoplasmic reticulum function. *J. Cell Biol.* **166,** 325–335 CrossRef Medline
52. Ellis, C. D., Macdiarmid, C. W., and Eide, D. J. (2005) Heteromeric protein complexes mediate zinc transport into the secretory pathway of eukaryotic cells. *J. Biol. Chem.* **280,** 28811–28818 CrossRef Medline
53. Fang, Y., Sugiura, R., Ma, Y., Yada-Matsushima, T., Umeno, H., and Kuno, T. (2008) Cation diffusion facilitator Cis4 is implicated in Golgi membrane trafficking via regulating zinc homeostasis in fission yeast. *Mol. Biol. Cell* **19,** 1295–1303 CrossRef Medline
54. Roh, H. C., Collier, S., Deshmukh, K., Guthrie, J., Robertson, J. D., and Kornfeld, K. (2013) ttm-1 encodes CDF transporters that excrete zinc from intestinal cells of *C. elegans* and act in a parallel negative feedback circuit that promotes homeostasis. *PLoS Genet.* **9,** e1003522 CrossRef Medline
55. Lye, J. C., Richards, C. D., Dechen, K., Paterson, D., de Jonge, M. D., Howard, D. L., Warr, C. G., and Burke, R. (2012) Systematic functional characterization of putative zinc transport genes and identification of zinc toxicosis phenotypes in *Drosophila melanogaster*. *J. Exp. Biol.* **215,** 3254–3265 CrossRef Medline
56. Gustin, J. L., Zanis, M. J., and Salt, D. E. (2011) Structure and evolution of the plant cation diffusion facilitator family of ion transporters. *BMC Evol. Biol.* **11,** 76 CrossRef Medline
57. Kambe, T., Tsuji, T., Hashimoto, A., and Itsumura, N. (2015) The physiological, biochemical, and molecular roles of zinc transporters in zinc homeostasis and metabolism. *Physiol. Rev.* **95,** 749–784 CrossRef Medline
58. Choi, S., Hu, Y. M., Corkins, M. E., Palmer, A. E., and Bird, A. J. (2018) Zinc transporters belonging to the Cation Diffusion Facilitator (CDF) family have complementary roles in transporting zinc out of the cytosol. *PLoS Genet.* **14,** e1007262 CrossRef Medline
59. Hu, Y. M., Boehm, D. M., Chung, H., Wilson, S., and Bird, A. J. (2019) Zinc-dependent activation of the Pho8 alkaline phosphatase in *Schizosaccharomyces pombe*. *J. Biol. Chem.* **294,** 12392–12404 CrossRef Medline
60. Saito, Y., Ihara, Y., Leach, M. R., Cohen-Doyle, M. F., and Williams, D. B. (1999) Calreticulin functions *in vitro* as a molecular chaperone for both glycosylated and nonglycosylated proteins. *EMBO J.* **18,** 6718–6729 CrossRef Medline
61. Watanabe, S., Amagai, Y., Sannino, S., Tempio, T., Anelli, T., Harayama, M., Masui, S., Sorrentino, I., Yamada, M., Sitia, R., and Inaba, K. (2019) Zinc regulates ERp44-dependent protein quality control in the early secretory pathway. *Nat. Commun.* **10,** 603 CrossRef Medline
62. Kambe, T. (2020) Metalation and maturation of zinc ectoenzymes: a perspective. *Biochemistry* **59,** 74–79 CrossRef Medline
63. Kambe, T. (2014) Methods to evaluate zinc transport into and out of the secretory and endosomal-lysosomal compartments in DT40 cells. *Methods Enzymol.* **534,** 77–92 CrossRef Medline
64. Kambe, T., and Andrews, G. K. (2009) Novel proteolytic processing of the ectodomain of the zinc transporter ZIP4 (SLC39A4) during zinc deficiency is inhibited by acrodermatitis enteropathica mutations. *Mol. Cell. Biol.* **29,** 129–139 CrossRef Medline
65. Nishito, Y., Tsuji, N., Fujishiro, H., Takeda, T. A., Yamazaki, T., Teranishi, F., Okazaki, F., Matsunaga, A., Tuschl, K., Rao, R., Kono, S., Miyajima, H., Narita, H., Himeno, S., and Kambe, T. (2016) Direct comparison of manganese detoxification/efflux proteins and molecular characterization of ZnT10 as a manganese transporter. *J. Biol. Chem.* **291,** 14773–14787 CrossRef Medline

Downloaded from http://www.jbc.org/ at Kyoto University on June 11, 2020

ASBMB

Detailed analyses of the crucial functions of Zn transporter proteins in alkaline phosphatase activation

Eisuke Suzuki, Namino Ogawa, Taka-aki Takeda, Yukina Nishito, Yu-ki Tanaka, Takashi Fujiwara, Mayu Matsunaga, Sachiko Ueda, Naoya Kubo, Tokuji Tsuji, Ayako Fukunaka, Tomohiro Yamazaki, Kathryn M. Taylor, Yasumitsu Ogra and Taiho Kambe

J. Biol. Chem. 2020, 295:5669-5684.
doi: 10.1074/jbc.RA120.012610 originally published online March 16, 2020

Access the most updated version of this article at doi: 10.1074/jbc.RA120.012610

Alerts:
- When this article is cited
- When a correction for this article is posted

Click here to choose from all of JBC's e-mail alerts

This article cites 65 references, 34 of which can be accessed free at
http://www.jbc.org/content/295/17/5669.full.html#ref-list-1

Downloaded from http://www.jbc.org/ at Kyoto University on June 11, 2020